

UNIVERSITY OF MICHIGAN



**REPAIR AND STRENGTHENING OF REINFORCED CONCRETE
BEAMS USING CFRP LAMINATES**

Volume 3: Behavior of Beams Strengthened For Bending

by

Antoine Naaman
Sang Yeol Park
Maria del Mar Lopez

Project Coordinator: Roger D. Till, MDOT
Project Advisor: Thomas D. Gillespie, GLCTTR

Report No. UMCEE 98 - 21
April, 1999

The University of Michigan
Department of Civil and Environmental Engineering
Ann Arbor, MI 48109-2125, USA

Technical Report Documentation Page

1. Report No. RC - 1372	2. Government Accession No.	3. Recipient's Catalog No.	
4. Title and Subtitle Repair and Strengthening of Reinforced Concrete Beams using CFRP Laminates. Volume 3: Behavior of Beams Strengthened for Bending		5. Report Date April, 1999	
7. Author (s) Antoine E. Naaman Sang Yeol Park Maria del Mar Lopez		6. Performing Organization Code UMCEE 98 - 21	
9. Performing Organization Name and Address The University of Michigan, Dept. of Civil and Env. Engineering 2340 G.G. Brown Bldg. Ann Arbor, MI 48109-2125		8. Performing Org Report No. RC - 1372	
12. Sponsoring Agency Name and Address Michigan Department of Transportation Construction and Technology Division P.O. Box 30049 Lansing, MI 48909		10. Work Unit No. (TRAIS)	
		11. Contract/Grant No.	
15. Supplementary Notes		13. Type of Report & Period Covered Research Report 1997-1998	
		14. Sponsoring Agency Code	
<p>16. Abstract</p> <p>Repair and strengthening techniques using glued-on carbon fiber reinforced plastic (CFRP) plates (also called sheets, tow-sheets, and thin laminates) form the basis of a new technology being increasingly used for bridges and highway superstructures.</p> <p>The study described in this report (Volumes 1 to 7) focused on the use of carbon fiber reinforced plastic (CFRP) laminates for repair and strengthening of reinforced concrete beams. Its primary objectives are: 1) to ascertain the applicability of CFRP adhesive bonded laminates for repair and strengthening of reinforced concrete beams; 2) to synthesize existing knowledge and develop procedures for implementation in the field; 3) to identify key parameters for successful design and implementation; and 4) to adapt this technique to the specific conditions encountered in the state of Michigan.</p> <p>This report consists of 7 volumes: Volume 1 – Summary Report Volume 2 – Literature Review Volume 3 – Behavior of Beams Strengthened for Bending Volume 4 – Behavior of Beams Strengthened for Shear Volume 5 – Behavior of Beams Under Cyclic Loading at Low Temperature Volume 6 – Behavior of Beams Subjected to Freeze-Thaw Cycles Volume 7 – Technical Specifications.</p> <p>The part of the investigation dealing with reinforced concrete beams strengthened in bending is described in this volume (volume 3), where the results are also analyzed, compared, and discussed. The experimental program comprised fourteen reinforced concrete T-beams. The test parameters included two levels of steel reinforcement ratio before strengthening, and up to four strengthening levels. Two commercially available strengthening systems were tested, the Sika CFRP plate system (CarboDur), and the Tonen CFRP sheet system. Other selective parameters investigated included two different concrete covers; two conditions of cover preparation, three different end anchorage systems of the glued-on sheets, and pre-loading pre-yielding of the beam prior to strengthening. Conclusions are drawn and some recommendations for design are suggested.</p>			
17. Keywords bond, carbon fiber, composites materials, laminates, rehabilitation, reinforced concrete, repair, strengthening systems		18. Distribution Statement No restrictions. This document is available to the public through the Michigan Department of Transportation	
19. Security Classification (report) Unclassified	20. Security Classification (Page) Unclassified	21. No. of pages	22. price

Michigan Department of Transportation - Technical Advisory Group

Roger D. Till, *Project Coordinator*
Materials and Technology Laboratories

David Juntunen
Materials and Technology Laboratories

Jon Reincke
Materials and Technology Laboratories

Glenn Bukoski
Construction

Steve Beck
Design

Raja Jildeh
Design

Michel Tarazi
Design

Steve O'Connor
Engineering Services

Sonny Jadun
Maintenance

John Nekritz
Federal Highway Administration

Great Lakes Center for Trucks and Transit Research

Thomas D. Gillespie, *Project Advisor*
University of Michigan Transportation Research Institute

University of Michigan - CEE Research Team

Antoine Naaman, *Project Director*

Sang Yeol Park, *Research Fellow*

Maria del Mar Lopez, *Graduate Research Assistant*

Luke R. Pinkerton, *Graduate Research Assistant*

UMCEE 98 - 21
MDOT Contract No: 96-1067BAB

Project Director: Antoine E. Naaman, UM
Project Coordinator: Roger D. Till, MDOT
Project Advisor: Thomas D. Gillespie, GLCTTR

August, 1998

key words:

adhesives
bending
bond
carbon fiber
composite materials
concrete
durability
epoxy
fatigue
freeze thaw
FRP sheets
low temperature
repair
rehabilitation
shear
strengthening systems

Department of Civil and Environmental Engineering
University of Michigan, 2340 G.G. Brown building
Ann Arbor, MI 48109-2125
Tel: 1-734-764-8495; Fax: 1-734-764 4292

The publication of this report does not necessarily indicate approval or endorsement of the findings, opinions, conclusions, or recommendations either inferred or specifically expressed herein, by the Regents of the University of Michigan, the Michigan Department of Transportation, or the Great Lakes Center for Trucks and Transit Research.

ACKNOWLEDGMENTS

The research described in this report was supported jointly by a grant from the Michigan Department of Transportation and the Great Lakes Center of Truck and Transit Research which is affiliated with the University of Michigan Transportation Research Institute. Matching funds for student tuition and for equipment were also provided by the University of Michigan.

The research team received valuable support, counsel, and guidance from the Technical Advisory Group. The support and encouragement provided by Roger Till, project coordinator representing the Michigan Department of Transportation, is deeply appreciated.

The authors are thankful to the Sika Corporation (Bob Pisha) for the donation of the Carbodur laminate as well as the Sikadur epoxy material. The partial contribution of Tonen Corporation with the MBrace composite strengthening system, and the help of Howard Kliger are also appreciated.

The opinions expressed in this report are those of the authors and do not necessarily reflect the views of the sponsors.

TABLE OF CONTENTS

ACKNOWLEDGMENTS	iii
PREFACE	vii
ABSTRACT	viii
1. GENERAL	1
2. EXPERIMENTAL PROGRAM.....	1
2.1. Test Parameters	3
2.2. Preparation of Test Beams.....	5
2.2.1. Concrete	5
2.2.2. CFRP Sheets	10
2.2.3. Reinforcing Bars.....	10
2.2.4. Fabrication of Test Beams.....	10
2.2.5. Preparation of Concrete Surface for Bond.....	14
2.2.6. Gluing CFRP Sheet or Plate	14
2.3. Data Acquisition and Test Procedure	15
3. ANALYSIS AND DISCUSSION OF TEST RESULTS.....	16
3.1. Steel Reinforcement Ratio and Strengthening Level.....	16
3.1.1. Reinforcement Ratio $0.27\rho_{max}$	16
3.1.2. Reinforcement Ratio $0.54\rho_{max}$	25
3.1.3. Influence of Strengthening Level _x	29
3.2. Influence of Strengthening System.....	36
3.3. Influence of Concrete Cover.....	41
3.4. Influence of End Anchorage.....	43
3.5. Influence of Surface Preparation.....	45
3.6. Influence of Loading History.....	47
3.7. Residual Strength of Beam after Failure.....	48
4. CONCLUSIONS	49
5. REFERENCES WITH SOURCE CLASSIFICATION	52
6. APPENDIX A: MOMENT CAPACITY CALCULATIONS	55

LIST OF FIGURES

FIGURE 1	TYPICAL CROSS SECTION AND LOADING ARRANGEMENT FOR BENDING TESTS	2
FIGURE 2	PARAMETERS FOR THE BENDING TESTS.....	8
FIGURE 3	CASTING OF CONCRETE OF TEST BEAMS	13
FIGURE 4	GLUING OF CFRP SHEET ON THE SOFFIT OF A BEAM.....	15
FIGURE 5	INSTRUMENTATION LAYOUT FOR THE BENDING TESTS.....	16
FIGURE 6	TENSILE FAILURE OF CFRP SHEET IN BEAM NO. 2	18
FIGURE 7	INTERFACIAL SHEAR FAILURE OF CONCRETE IN BEAM NO. 3.....	19
FIGURE 8	LOAD-STRAIN CURVES OF BEAM NO. 3	20
FIGURE 9	LOAD-STRAIN CURVES OF BEAM NO. 4	20
FIGURE 10	LOAD-DEFLECTION CURVES OF BEAMS WITH REINFORCEMENT RATIO, $0.27\rho_{MAX}$, FOR DIFFERENT STRENGTHENING LEVELS	21
FIGURE 11	LOAD-STRAIN CURVES OF REINFORCING BAR.....	22
FIGURE 12	DEFLECTION-STRAIN CURVES OF REINFORCING BAR.....	22
FIGURE 13	LOAD-STRAIN CURVES OF CONCRETE IN TOP FLANGE.....	23
FIGURE 14	DEFLECTION-STRAIN CURVES OF CONCRETE IN TOP FLANGE.....	23
FIGURE 15	LOAD-STRAIN CURVES OF CFRP SHEET	24
FIGURE 16	DEFLECTION-STRAIN CURVES OF CFRP SHEET.....	25
FIGURE 17	TENSILE RUPTURE AND DELAMINATION OF CFRP SHEET IN BEAM NO. 6	26
FIGURE 18	LOAD-DEFLECTION CURVES OF BEAMS WITH REINFORCEMENT RATIO, $0.54\rho_{MAX}$, AT TWO STRENGTHENING LEVELS	27
FIGURE 19	LOAD-STRAIN OF REINFORCING BAR OF BEAMS WITH REINFORCEMENT RATIO, $0.54\rho_{MAX}$, AT TWO STRENGTHENING LEVELS	27
FIGURE 20	DEFLECTION-STRAIN CURVES OF REINFORCING BAR OF BEAMS WITH REINFORCEMENT RATIO, $0.54\rho_{MAX}$, AT TWO STRENGTHENING LEVELS.....	28
FIGURE 21	LOAD-STRAIN CURVES OF CFRP SHEET OF BEAMS WITH REINFORCEMENT RATIO, $0.54\rho_{MAX}$, AT TWO STRENGTHENING LEVELS	28
FIGURE 22	DEFLECTION-STRAIN CURVES OF FRP SHEET OF BEAMS WITH REINFORCEMENT RATIO, $0.54\rho_{MAX}$, AT TWO STRENGTHENING LEVELS	29
FIGURE 23	RELATIONSHIP BETWEEN ULTIMATE LOAD AND STRENGTHENING LEVEL.....	33
FIGURE 24	INCREMENT OF ULTIMATE LOAD VERSUS STRENGTHENING LEVEL.....	33
FIGURE 25	INCREASE IN RATIO OF ULTIMATE LOAD VERSUS STRENGTHENING LEVEL.....	34
FIGURE 26	ULTIMATE DEFLECTION VERSUS STRENGTHENING LEVEL	34
FIGURE 27	TENSILE FORCE OF CFRP SHEET VERSUS STRENGTHENING LEVEL	35
FIGURE 28	SHEAR STRESS OF CONCRETE AT DELAMINATION OF CFRP SHEET	35
FIGURE 29	INTERFACIAL SHEAR FAILURE (DELAMINATION) OF CONCRETE IN BEAM NO.8	37
FIGURE 30	INTERFACIAL SHEAR FAILURE OF CONCRETE IN BEAM NO.8-1	37
FIGURE 31	LOAD-DEFLECTION CURVES FOR DIFFERENT STRENGTHENING SYSTEMS.....	38
FIGURE 32	LOAD-STRAIN CURVES OF REINFORCING BAR.....	38
FIGURE 33	DEFLECTION-STRAIN CURVES OF REINFORCING BAR.....	39
FIGURE 34	LOAD-STRAIN CURVES OF CONCRETE.....	39
FIGURE 35	DEFLECTION-STRAIN CURVES OF CONCRETE	40
FIGURE 36	LOAD-STRAIN CURVES OF CFRP SHEET	40
FIGURE 37	DEFLECTION-STRAIN CURVES OF CFRP SHEET.....	41
FIGURE 38	INTERFACIAL BOND FAILURE OF CFRP SHEET IN BEAM NO. 9	42
FIGURE 39	LOAD-DEFLECTION CURVES OF BEAMS WITH DIFFERENT CONCRETE COVER.....	42
FIGURE 40	INTERFACIAL SHEAR FAILURE OF CONCRETE IN BEAM NO. 10	43
FIGURE 41	INTERFACIAL SHEAR FAILURE OF CONCRETE IN BEAM NO. 14	44
FIGURE 42	LOAD-DEFLECTION CURVES OF BEAMS WITH DIFFERENT ANCHORAGE.....	44
FIGURE 43	LOAD-DEFLECTION CURVES OF BEAMS WITH DIFFERENT SURFACE PREPARATION.....	45
FIGURE 44	INTER-LAMINAR SHEAR FAILURE OF BEAM NO. 11.....	46
FIGURE 45	LOAD-DEFLECTION CURVES OF BEAMS WITH DIFFERENT LOADING HISTORY.....	46
FIGURE 46	CONDITION OF BEAM NO. 13 FAILED BY DELAMINATION BEFORE RE-TESTING	48
FIGURE 47	LOAD-DEFLECTION CURVES OF BEAM NO. 13	49

LIST OF TABLES

TABLE 1A PARAMETERS AND VARIABLES FOR THE BENDING TESTS($F'c=55.2$ MPA)	6
TABLE 1B TEST PARAMETERS AND VARIABLES FOR BENDING TEST ($F'c= 55.2$ MPA)	7
TABLE 2 MIX PROPORTIONS OF CONCRETE	9
TABLE 3 COMPRESSIVE STRENGTH OF CONCRETE AND AGE OF TEST BEAMS	9
TABLE 4 PROPERTIES OF CFRP SHEETS (PLATES) AND ADHESIVES.....	12
TABLE 5 YIELD STRENGTH AND ELASTIC MODULUS OF REINFORCING BARS AS TESTED	13
TABLE 6 SUMMARY OF TEST RESULTS OF BENDING TEST.....	17
TABLE 7 SUMMARY OF TEST RESULTS OF BEAMS WITH DIFFERENT STRENGTHENING LEVELS.....	31

PREFACE

This project titled: "*Repair and Strengthening of Reinforced Concrete Beams using CFRP Laminates*" is aimed at providing experimental verification and recommendations for implementation of a new technology, in which thin fiber reinforced plastic laminates are glued-on the surface of concrete beams in order to strengthen them.

The primary objectives of the project were:

- To ascertain the applicability of Carbon Fiber Reinforced Plastic (CFRP) glued-on plates for repair and strengthening of concrete beams;
- To synthesize existing knowledge and develop procedures for implementation in the field;
- To adapt this technique to the specific conditions encountered in the state of Michigan.

The project consisted of 8 tasks as follows:

- A report containing a literature review and a comprehensive synthesis of the latest state of knowledge on the glued-on FRP technique (Task 1);
- Laboratory testing and verification of the selected CFRP glued-on technique according to the proposed experimental program: bending (Task 2), shear (Task 3), freeze-thaw (Task 4), temperature and high cyclic amplitude load (Task 5);
- An interim and final report summarizing the experimental results (Task 6). The interim report will cover the bending and freeze-thaw tests;
- A summary of field specifications and "how to" details for implementation in field applications;
- Guidelines for design based on the experience developed from the experimental work (Task 7);
- Field monitoring of application of the technique to one bridge selected by MDOT (Task 8a);
- Bridge testing before and after application of the glued-on plate (Task 8b to be conducted by professor A. Nowak, U of M)

This report summarizes the experimental program of beams strengthened for bending as per Task 2.

ABSTRACT

Repair and strengthening techniques using glued-on carbon fiber reinforced plastic (CFRP) plates (also called sheets, tow-sheets, and thin laminates) form the basis of a new technology being increasingly used for bridges and highway superstructures.

The study described in this report is part of a larger investigation on the use of carbon fiber reinforced plastic (CFRP) sheets for repair and strengthening of reinforced and prestressed concrete beams. Its primary objectives are: 1) to ascertain the applicability of CFRP glued-on plates for repair and strengthening of concrete beams, 2) to synthesize existing knowledge, 3) to identify optimum parameters for successful implementation, 4) to develop procedures for implementation in the field, and 5) to adapt the technique to the specific conditions encountered in the state of Michigan.

The experimental program includes four main parts: 1) tests of RC beams strengthened in bending; 2) tests of RC beams strengthened in shear; 3) freeze-thaw tests of strengthened beams followed by their test in bending; and 4) tests in bending and shear of strengthened beams under low temperature (-29°C) and high amplitude cyclic loading.

The part of the investigation dealing with reinforced concrete beams strengthened in bending is described in this report, where the results are also analyzed, compared, and discussed. The experimental program comprised fourteen reinforced concrete T-beams. The test parameters included two levels of steel reinforcement ratio before strengthening, and up to four strengthening levels. Two commercially available strengthening systems were tested, the Sika CFRP plate system (CarboDur), and the Tonen CFRP sheet system. Other selective parameters investigated included two different concrete covers; two conditions of cover preparation, three different end anchorage systems of the glued-on sheets, and pre-loading pre-yielding of the beam prior to strengthening. Conclusions are drawn and some recommendations for design are suggested.

Since the plate glued-on technique applies to plain, reinforced and prestressed concrete structures, as well as steel and timber structures, the experience gained during this project and the technology transfer developed should have a much wider impact and should influence a wide range of future applications.

1. GENERAL

Technique of external epoxy-bonded steel plates have been used successfully to increase the strength of girders in existing bridges and buildings. High strength Fiber Reinforced Polymer (FRP) composites are used as an extension of the steel plating method, offering the advantages of composite materials such as non-corrosion, light weight, and unlimited delivery length, thus eliminating the need for joints. FRP sheets or plates may be needed to improve the maximum load capacity and reduce the vertical deflection at service of bridge structures. Also, their use tends to limit the width of cracks and improve their distribution in concrete beams.

The study described in this report is part of a larger investigation on the use of carbon fiber reinforced plastic (CFRP) sheets for repair and strengthening of reinforced concrete beams. Its primary objectives are: 1) to ascertain the applicability of CFRP glued-on plates for repair and strengthening of concrete beams, 2) to synthesize existing knowledge and develop procedures for implementation in the field, and 3) to adapt the technique to the specific conditions encountered in the state of Michigan.

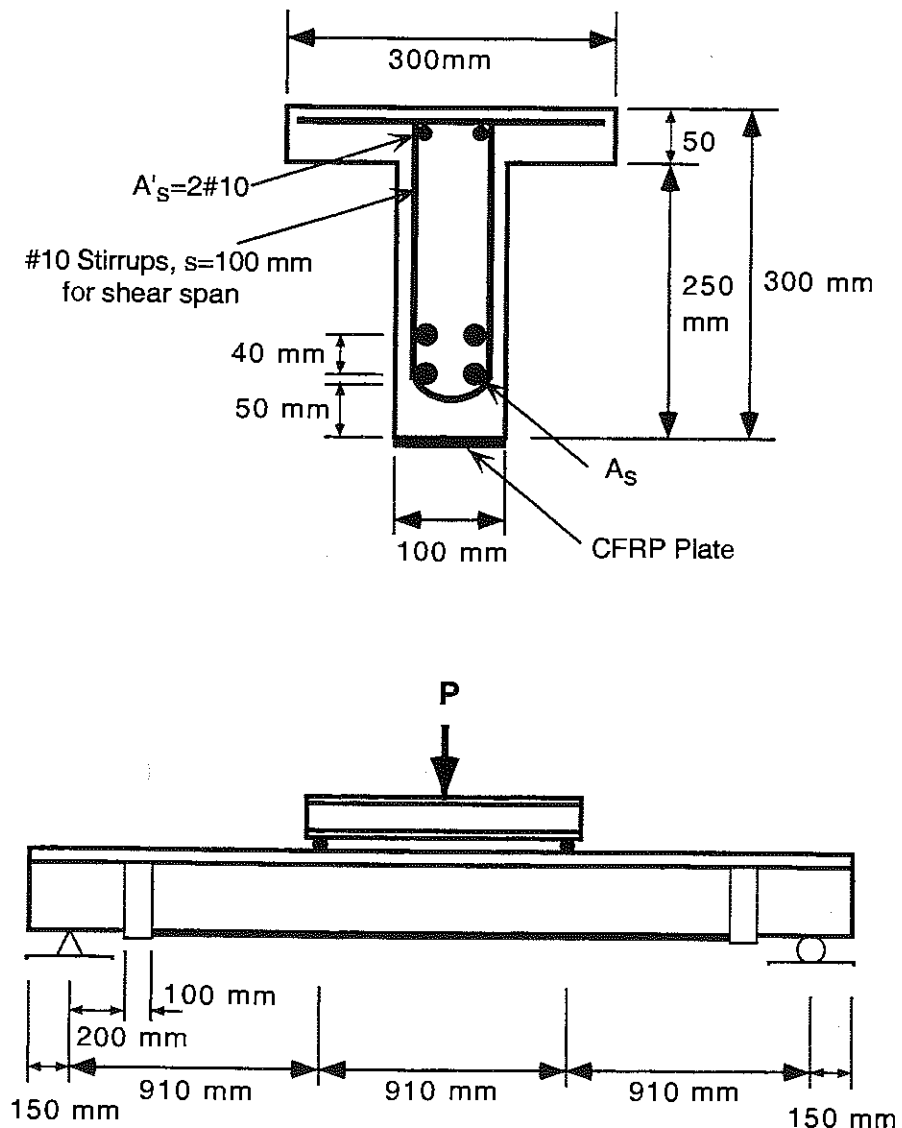
The experimental program includes: 1) tests of reinforced concrete (RC) beam strengthened in bending; 2) tests of RC beams strengthened in shear; 3) freeze-thaw tests of strengthened beams followed by their test in bending; and 4) tests in bending and shear of strengthened beams under low temperature (-29 C) and high amplitude cyclic loading.

The part of the investigation dealing with reinforced concrete beams strengthened in bending is described in this report, where the results are also analyzed, compared, and discussed.

2. EXPERIMENTAL PROGRAM

The experimental program for bending tests comprised fourteen reinforced concrete T beams. The loading arrangement and cross sectional dimensions are shown in Figure 1. All beams were 300 mm deep and 3.0 m long. In most cases, concrete cover for reinforcing steel was kept at 50 mm. To investigate the flexural

behavior, a four-point bending test set-up was used. For bending, the CFRP sheet or plate ran along the bottom of a beam extreme tensile fiber as shown in Figure 1. Normally, at its two ends, a 100 mm wide U-shaped anchorage sheet with fibers normal to the axis of the beam was wrapped around in order to provide additional anchorage and minimize the chances of peeling from the ends of CFRP sheets. Before application of the glued-on CFRP sheets or plate, all beams were pre-cracked by pre-loading to about 60% of their ultimate design load, 50 kN and 89 kN for the beams with the steel reinforcement ratios $0.27\rho_{\max}$ and $0.54\rho_{\max}$, respectively. This is to simulate actual condition of cracked reinforced concrete beams at the time the strengthening system is applied.



Throughout the experimental study, particular effort was placed at observing the type of failure and understanding its mechanisms. Also, the applied load, corresponding deflection, as well as the strains of reinforcing bars and CFRP sheet or plate were measured.

2.1 Test Parameters

A number of test parameters were initially proposed by the research team and further refined after discussion with the Technical Advisory Group of the project. These parameters and related experimental variables for the bending tests are summarized in Table 1 and illustrated in Figure 2.

The decision was made to consider two different reinforcement ratios corresponding approximately to one third and two thirds the maximum reinforcement ratio (ρ_{max}) recommended by the AASHTO Code, sixteenth edition. Computations of reinforcement ratios and selection of reinforcing bars were carried out on the basis that the concrete compressive strength, obtained from cylinder tests, would be 35 MPa. Other parameters were then selected as shown in Table 1a. However, the beams were prepared in factory in a precast concrete plant and were steam cured; although the specified compressive strength of concrete was 35 MPa, the actual compressive strength at time of testing averaged about 56 MPa. Thus back-calculation was carried out to lead to the actual test parameters described in Tables 1a and 1b (see Appendix A for detailed calculations). These parameters should be considered the real parameters of the test program. In addition, the actual value for yield strength of the reinforcing bars was also used for this back calculation.

The test parameters included the existing steel reinforcement ratio before strengthening, and the strengthening level. For each steel reinforcement ratio, a control beam was tested and compared with CFRP glued-on beams having different strengthening levels. Beams No. 1 and No. 5 were control beams with steel reinforcement ratios of $0.27\rho_{max}$ and $0.54\rho_{max}$. The maximum steel reinforcement ratio, ρ_{max} , was defined as per the AASHTO Code to represent 75% of the balanced

ratio. The strengthening level (i.e., the number of CFRP sheets, if more than one) was determined assuming that (except for beam 8-1) the total reinforcement of steel and CFRP will lead to a moment resistance not exceeding the moment corresponding to the maximum reinforcement ratio allowed for the beam by AASHTO or ACI, assuming beams with reinforcing bars only.

Two strengthening systems were tested: 1) the Sika CFRP plate system (CarboDur), and 2) the Tonen CFRP sheet system. The characteristics of these two systems are described in Section 2.2.2. The Tonen system was used throughout except for two beams, Beams No. 8 and 8-1. For Beam No. 8, the glued-on Sika CFRP plate had a width of 40 mm, which is equivalent in tensile strength to 2 layers of Tonen CFRP sheets (Forca Tow sheet). Following testing, Beam No. 8 was in very good shape even after the interfacial shear failure of concrete. There was no spalling of concrete cover even though the reinforcing bars had yielded and the 40 mm wide CFRP plate was completely delaminated. Beam No. 8 was later re-used as Beam No. 8-1, this time with a CFRP plate 100 mm wide to study different bond widths and strengthening levels.

For one selected set of parameters, two different concrete covers and cover conditions were investigated to study the influence of concrete cover on strengthening effect and mode of failure. Beam No. 12 had only a 25 mm concrete cover compared to the normal clear cover of 50 mm of the other beams. Beam No. 9 also had an initial 25 mm clear concrete cover to which additional 25 mm repair mortar cover (Sika Top 122 Plus) was added to simulate damaged concrete in real beams.

To evaluate different anchorage systems, three different anchorage conditions were provided. Beam No. 10 had extended end anchorage which means that the glued-on CFRP sheets were extended up to about 50 mm from the supports, without adding the U-shaped wrapped-around end anchorage.

Beam No. 14 had neither a wrapped end anchorage nor an extended end anchorage. All other beams strengthened with Tonen sheets had, at both ends, a 100 mm wide U-shaped wrapped-around end anchorage perpendicular to the longitudinal CFRP sheets. The beam with strengthened with the Sika system (8,8-1) did not have a wrapped end anchorage.

Beam No. 11 was pre-loaded beyond yielding of steel reinforcing bars, to about 180 kN, to investigate the influence of loading history before the application of CFRP plate. The permanent deflection and maximum crack width at unloading in the pre-cracked beam were 25 mm and 0.9 mm, respectively.

For all beams except for Beam No. 13, the concrete surface to be glued on was prepared, for better bond, by grinding with a disk grinder according to the recommendations of the supplier of the strengthening system used. For Beam No. 13, the surface of concrete was simply cleaned with a vacuum cleaner and wiped with a clean cloth to remove any dust.

2.2 Preparation of Test Beams

2.2.1 Concrete

The test beams were supplied by a precast concrete manufacturer, according to the design specifications. Portland cement Type-III cement, natural sand, and crushed limestone aggregates with a maximum size of 12.5 mm were used for the concrete. The mix proportions of the concrete as provided by the supplier are presented in Table 2.

Table 1a Parameters and variables for the bending tests ($f_c=55.2$ MPa).

Beam No.	Test parameter	Reinforcement ratio, ρ	A_s (used) mm ²	M_n/M_{max} %	Forca Tow sheet FTS-C1-30	Strengthening ratio ¹ % (ρ) ²	CarboDur strip (1 layer)	Strengthening ratio ¹ % (ρ) ²
1					0	0 (29)		
2		0.27 ρ_{max}	2#10 2#13 $A_s=400$	29	1 layer	12 (41)		
3	Steel reinforcement ratio				2 layers	24 (52)		
4	&				4 layers	47 (75)		
5	Strengthening level				0	0 (57)		
6		0.54 ρ_{max}	4#16 $A_s=800$	57	1 layer	12 (68)		
7					2 layers	24 (80)		
8		0.54 ρ_{max}	4#16 $A_s=800$	57			width=40 mm	22 (78)
8-1	Different system (Sika)	0.54 ρ_{max}	4#16 $A_s=800$	57			width=100 mm	60 (113)
9	Repaired concrete over	0.54 ρ_{max}	4#16 $A_s=800$	57	2 layers	24 (80)		
10	Extended end anchorage	0.54 ρ_{max}	4#16 $A_s=800$	57	2 layers	24 (80)		
11	Pre-loading	0.54 ρ_{max}	4#16 $A_s=800$	57	2 layers	24 (80)		
12	Concrete cover depth 25 mm	0.54 ρ_{max}	4#16 $A_s=800$	57	2 layers	22 (78)		
13	Cleaned surface	0.54 ρ_{max}	4#16 $A_s=800$	57	2 layers	24 (80)		
14	No anchorage	0.54 ρ_{max}	4#16 $A_s=800$	57	2 layers	24 (80)		

Note: 1: $M_{FRP}/M_{max} \times 100$

2: $(M_{As} + M_{FRP})/M_{max} \times 100$, $M_{max} = M_n$ (when $A_s = A_{smax}$), ($f_c=55.2$ MPa, $f_y=455$ MPa, $A_{smax}=1490$ mm²)

All the above values are calculated

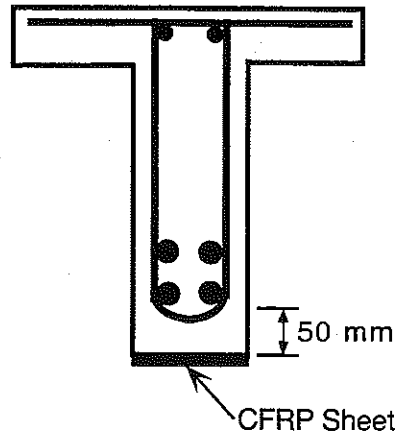
Table 1b Test parameters and variables for bending test ($f_c = 55.2$ MPa)

Beam No.	Test parameter	Reinforcement ratio, ρ	A_s (used) mm ²	Effective depth (mm)	Forca Tow sheet FTS-C1-30	Strengthening ratio ¹ % (ρ) ²	CarboDur strip (1 layer)	Strengthening ratio ¹ % (ρ) ²
1					0	0 (29)		
2		0.27 ρ_{max}	2#10 2#13 $A_s=400$	$d_s=235$ $d_f=305$	1 layer	41 (41)		
3					2 layers	81 (52)		
4					4 layers	160 (75)		
5				$d_s=227$	0	0 (57)		
6		0.54 ρ_{max}	4#16 $A_s=800$	$d_f=305$	1 layer	21 (68)		
7					2 layers	41 (80)		
8		0.54 ρ_{max}	4#16 $A_s=800$	$d_s=227$ $d_f=305$			width= 40 mm	39 (78)
8-1		0.54 ρ_{max}	4#16 $A_s=800$				width= 100 mm	100 (113)
9		0.54 ρ_{max}	4#16 $A_s=800$		2 layers	41 (80)		
10		0.54 ρ_{max}	4#16 $A_s=800$	$d_s=227$ $d_f=305$	2 layers	41 (80)		
11		0.54 ρ_{max}	4#16 $A_s=800$		2 layers	41 (80)		
12		0.54 ρ_{max}	4#16 $A_s=800$	$d_s=227$ $d_f=279$	2 layers	37 (78)		
13		0.54 ρ_{max}	4#16 $A_s=800$	$d_s=227$ $d_f=305$	2 layers	41 (80)		
14		0.54 ρ_{max}	4#16 $A_s=800$		2 layers	41 (80)		

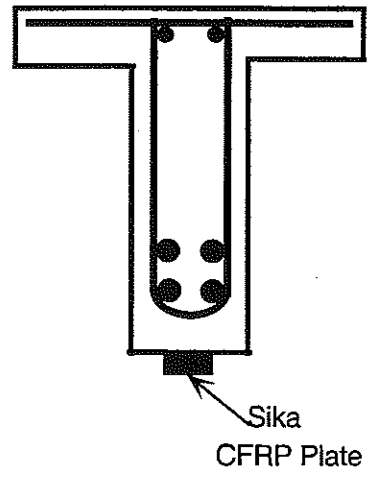
Note: 1: $(M_{(A_s+FRP)} - M_{As, (control)}) / M_{As, (control)}$ x100, based on the assumption of CFRP tensile failure

2: $(M_{As} + M_{FRP}) / M_{max, x100}$, $M_{max} = M_n$ (when $\rho = \rho_{max}$), ($f_c = 55.2$ MPa, $f_y = 455$ MPa, $A_{smax} = 1490$ mm²)

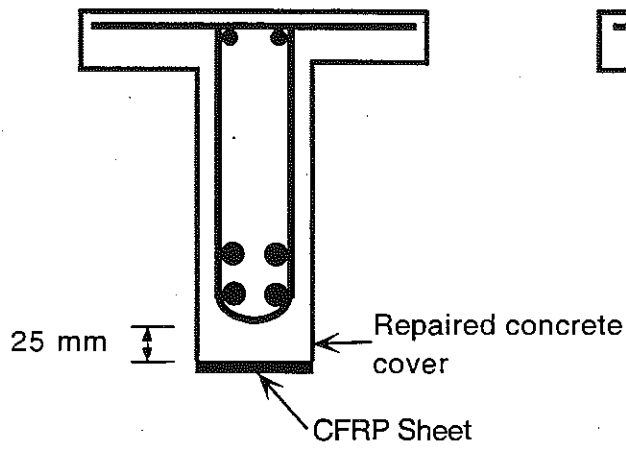
All the above values are calculated



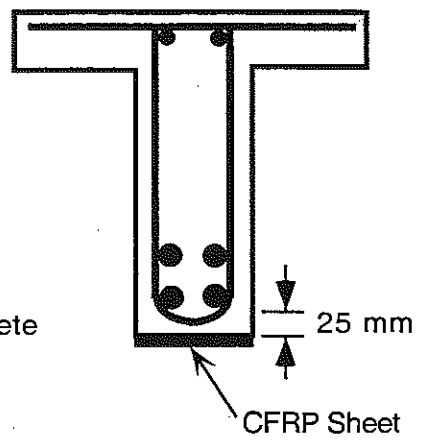
Normal concrete cover



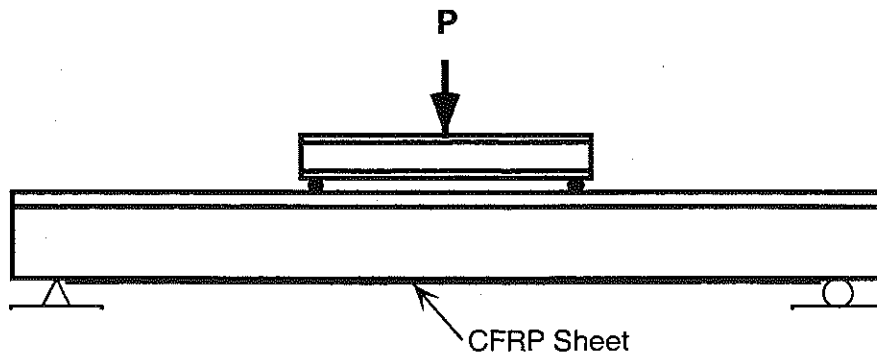
Different system



Repaired concrete cover



Concrete cover depth



Extended end anchorage

Table 2 Mix proportions of concrete.

Materials	Weight Ratio to Cement	Batch weight Kg-f/m ³
Type-III cement	1	418
Water	0.38	160
Sand (2S)	1.50	626
Coarse aggregate (26-A)	2.54	1062
Plasticizer (400N)	0.13	54
Air entrainer (AE-90)	0.035	15

The properties of the fresh concrete mixture were as follows;

- Air content : 6 %
- Slump: 100 mm
- Concrete unit weight: 22.3 kN/m³

Table 3 Compressive strength of concrete and age of test beams.

Batch No.	Age of concrete, day	Compressive strength of concrete, MPa	Test beam No.	Age of test beam, days
1	0.75*	32.1	8, (8-1)	86, (129)
	85	56.7	13	84
2	0.75*	30.8	6	29
	29	54.4	14	80
3	0.75*	28.3	5	77
	83	54.0	10	78
4	0.75*	28.0	7	28
	29	55.1	11	141
5	3	43.9	3	74
	81	58.8	4	73
6	0.75*	25.8	1	64
	78	51.9	2	65
7	0.75*	34.3	9	125
	77	55.5	12	77

* Steam cured concrete cylinders tested at 18 hours.

Note: Number of cylinders = 7 batches x 4 ea. = 28; 2 beams/batch = 14 beams.

Since the beams were steam cured, their average compressive strength obtained from two cylinder tests was measured at 18 hours (except for beam 5) and is given in Table 3. Also given in Table 3, is the average two-cylinders compressive strength of the concrete matrix at about the same time of testing for each beam. Difference in time is considered not significant. On the average, the compressive strength was about 55.2 Mpa.

2.2.2 CFRP Sheets

For strengthening of the test beams, the Forca Tow Sheet (Tonen CFRP sheet) supplied by Master Builders as part of the MBrace system (MB CF 130) and the CarboDur plate (Sika CFRP plate) with the corresponding epoxy adhesive (MBrace Saturant for the MBrace system and Sikadur 30 for the Sika system) of the same system were used. The properties of the materials in the two systems are summarized in Table 4. Values were provided by the manufacturers. According to the manufacturer, the tensile stress-strain curve of the CFRP sheet or plate is linear elastic up to failure.

2.2.3 Reinforcing Bars

The steel reinforcing bars used had a diameter of No. 10, No. 13, and No. 16 and were of Grade 400 corresponding to a minimum yield strength of 410 MPa with a tensile modulus of 200 GPa. Table 5 presents the actual yield strengths and elastic moduli obtained from direct tension tests carried out in this study on samples of bars.

2.2.4 Fabrication of Test Beams

All beams were fabricated in a precast concrete plant and delivered to the test laboratory with a number of additional cylinders for testing the concrete compressive strength. All test beams had four longitudinal reinforcing bars, placed in two rows, two in the lower row at a center distance of 60 mm from the bottom fiber of concrete, and two in the upper row with a center to center distance of 38 mm from the lower row. For each beam, two strain gages were attached on the

lower two reinforcing bars by the research team before assembling the reinforcement cage. All beams had 50 mm deep clear concrete cover from the bottom fiber except for Beam No. 12, which had 25 mm deep clear concrete cover.

Table 5 Yield strength and elastic modulus of reinforcing bars as tested.

Reinforcing bar		Yield stress MPa	Elastic modulus GPa
No. 10	#10-1	516	196
	#10-2	492	201
	#10-3	507	201
	Average	505	199
No. 13	#13-1	427	172
	#13-2	431	187
	#13-3	424	-
	Average	427	175
No. 16	#16-1	452	190
	#16-2	450	201
	#16-3	454	184
	Average	452	192

Table 4 Properties of CFRP sheets (plates) and adhesives.

Supplier		Tonen			Sika
System		Forca Tow Sheet			CarboDur
Type	FTS-C1-20	FTS-C1-30 (MBrace CF 130)	FTS-C5-30	CarboDur Strip	
CFRP Sheet	Tensile Strength, N/mm GPa	383 3.48	574 3.48	487 2.94	2868 2.40
	Tensile Modulus, kN/mm GPa	25.4 228	38.5 228	61.3 372	178.6 150
	Thickness ¹ , mm	0.11	0.17	0.17	1.19
	Elongation, %	1.5	1.5	0.8	1.4
	Width, mm	500			50, 80, 100
Length, m	Unlimited			Up to 250	
Epoxy	Type	FR-E3P	MBrace saturant	FR-E3PW	Sikadur 30
	Application temperature, °C	Standard	10-38	Winter	≥4
	Tensile strength, MPa		78		24.8
	Elastic Modulus, GPa				4.48
	Elongation, %				1
	Shear strength, MPa				24.8
	Shrinkage				0.0004
	Pot Life, min.	40	110	20	70
	Viscosity, cps	20,000	20,000	10,000	
	Type	Standard, Summer, Winter, Penetrative, Summer damp surface, Winter damp surface			No Primer

1: Total cross sectional area of fibers per inch.

To ensure flexural failure, sufficient stirrups designed according to AASHTO code were provided for all beams. Two-leg stirrups (closed with extended ends) made of 10 mm reinforcing bar were placed at a spacing of 100 mm and 200 mm within the shear span and constant moment span of the test beam, respectively. Figure 3 shows the casting of concrete of the test beams.

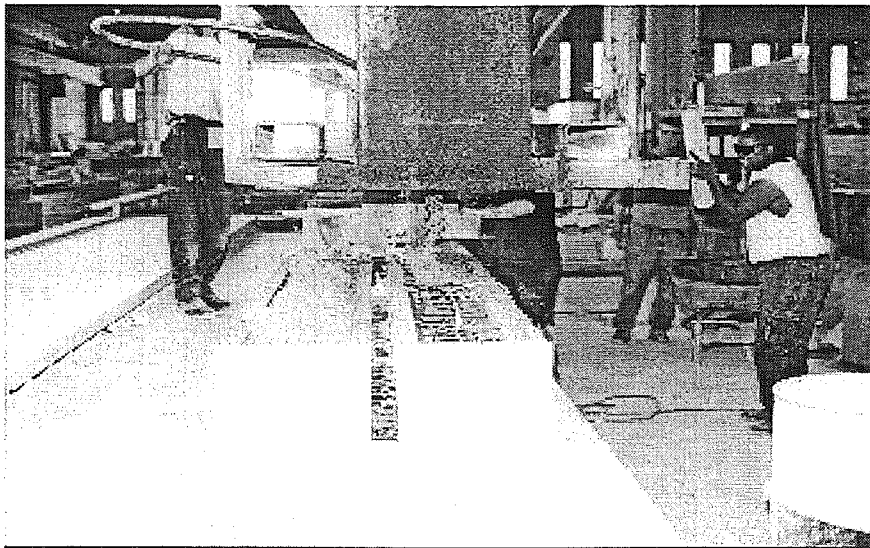


Figure 3 Casting of concrete of test beams.

2.2.5 Preparation of Concrete Surface for Bond

For the preparation of concrete surface to be glued on, two methods, steel brushing and disk grinding, were initially proposed to the supplier of the strengthening system. Of the two methods, the disk grinding method was recommended by the system supplier, after visual check of the surface substrate. The concrete surface was ground enough to remove laitance and show the open texture of the aggregates. After grinding, the dust was removed by brushing and vacuum cleaning the surface. Generally, the surface to be coated with the epoxy resin was even (level) without any roughness or formwork marks larger than 1.0 mm. To evaluate a different surface condition, the bottom surface of Beam No. 13 was simply wiped with a clean cloth and vacuumed without any disk grinding.

2.2.6 Gluing CFRP Sheet or Plate

The Forca Tow (Tonon) sheets and CarboDur (Sika) plates were cut to proper lengths using a sharp blade and a disk cutter, respectively. The CFRP sheet or plate was wiped with a clean cloth before starting application, in order to remove soiling as well as carbon dust.

The adhesives components were mixed according to the technical data sheet provided by the system supplier. Tonon epoxy resin was so sticky that mixing by hand was not easy. After first opening of the bucket, Tonon epoxy resin was so hardened from the surface that uniform mixing was very difficult because of hardened lumps and high viscosity. Sika epoxy was mixed in uniform consistency without any difficulties. It was like cement mortar with very low viscosity.

For the Tonon strengthening system, the primer and epoxy adhesive were applied using a roller similarly to the commercial specifications. The application of the adhesive using a roller, to form a layer of uniform thickness, was not easy because of its high viscosity. To press the CFRP sheet into the adhesive, a non-stick paper was placed between the CFRP sheet and the roller, and a harder roller was utilized. Figure 4 shows the gluing of the Tonon CFRP sheet on the soffit of a beam.

For the Sika strengthening system, a trowel was used to apply the epoxy adhesive to the surface of beam soffit and CFRP plate. To press CFRP plate into the epoxy adhesive, a hard roller was used forcing out the adhesive from the plate sides.

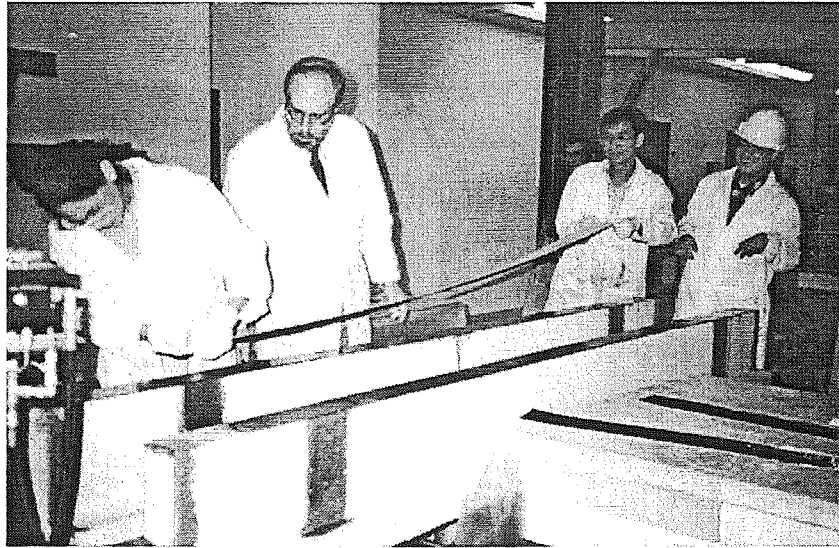


Figure 4 Gluing of CFRP sheet on the soffit of a beam.

2.3 Data Acquisition and Test Procedure

Figure 5 shows the instrumentation layout for the bending tests. A computer based data acquisition system (Megadack System) was used to measure load and deflection as well as strains of the steel reinforcing bars and the CFRP sheet or plate.

Each test beam was loaded monotonically up to failure using displacement control at a loading rate of 0.13 mm per second by the Instron loading machine having a capacity of 450 kN. Each beam was pre-loaded to about 8.9 kN before testing to remove any residual stress and deformation in the test beam and stabilize the instrumentation. At every 8.9 kN interval, loading was temporarily stopped to mark cracks. The following data was obtained every second by the data acquisition system: (1) load and deflection from the Instron loading machine, (2) strains of the reinforcing bars at midspan, (3) strains of the CFRP sheet or plate at the middle and both ends of span, and (4) deflections from the LVDTs at mid span.

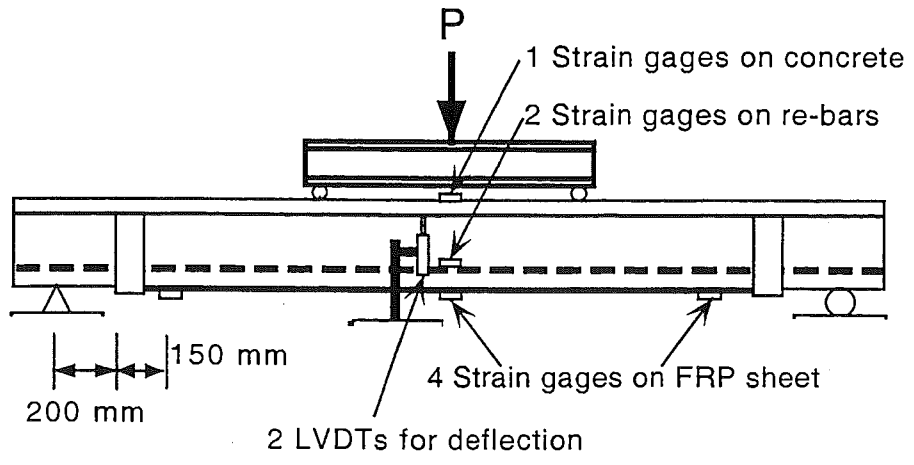


Table 6 Summary of test results of bending test

Beam No.	Test parameter	Reinforcement ratio	No. of CFRP layer	Failure mode ¹	Ultimate load kN	Strengthening ratio ² % () ³	Ultimate deflection mm
1	Steel reinforcement ratio & strengthening level	0.27 ρ_{max}	0	Steel yielding	114.8	0	164
2			1	CFRP rupture	135.0	18 (41)	83
3			2	Interface failure	140.4	22 (81)	56
4			4	Interface failure	160.7	40 (160)	49
5		0.54 ρ_{max}	0	Steel yielding	188.0	0	88
6			1	Interface failure	209.9	12 (21)	77
7			2	Interface failure	222.0	16 (41)	51
8	Different system (Sika)		40 mm	Interface failure	209.2	11 (39)	46
8-1			100 mm	Interface failure	250.9	33 (100)	41
9	Repaired concrete cover	0.54 ρ_{max}	2	Interface bond failure	208.2	11 (41)	73
10	Extended end anchorage			Interface failure	220.4	17 (41)	59
11	Pre-loading			Inter-laminar failure	226.2	20 (41)	119
12	Concrete cover depth			Interface failure	221.2	18 (37)	69
13	Cleaned surface			Interface failure	230.8	23 (41)	60
14	No anchorage			Interface failure	215.1	14 (41)	57

1: Steel yielding: Compression failure of top concrete long after reinforcement yielding
CFRP rupture: Tensile failure of CFRP sheet

Interface failure: Tensile failure of concrete just above the epoxy adhesive.

Interface bond failure: Interfacial shear failure of concrete between the repair mortar and the existing concrete

Interface bond failure: Interfacial bond failure between the repair mortar and the existing concrete

Inter-laminar failure: Inter-laminar shear failure between glued-on CFRP sheets

2: Actual strengthening ratio compared to control beam (Beam No. 1 or No. 5)

3: Design strengthening ratio compared to control beam based on the assumption of CFRP tensile failure (see Table 1b)

In their failure modes, Beam No. 2 failed by the tensile failure of CFRP sheet and Beams No. 3, and No. 4 failed by interfacial shear failure of the concrete (delamination) just above the epoxy adhesive. On the other hand, the control beam, Beam No. 1, failed by compression failure of the concrete in the top flange long after yielding of the steel reinforcing bars, which is a typical failure mode in conventional under-reinforced concrete beams. The CFRP sheets in the strengthened beams inhibited the growth of large cracks, which had occurred in the control beam, by leading to a better crack distribution with smaller crack widths and spacing. This can help to protect reinforcement from further corrosion.

In Beam No. 2, which failed by the tensile failure of CFRP sheet, the glued CFRP sheet was ruptured piece by piece (strip by strip) continuously over the length. Figure 6 shows the tensile failure of CFRP sheet observed in Beam No.2. In this failure mode, unlike the beams that failed by interfacial shear failure of concrete, there were no pieces of concrete cover spalled off from the beam. In other cases, interfacial shear failure of concrete is more likely to occur between the surface of concrete and the CFRP laminates.

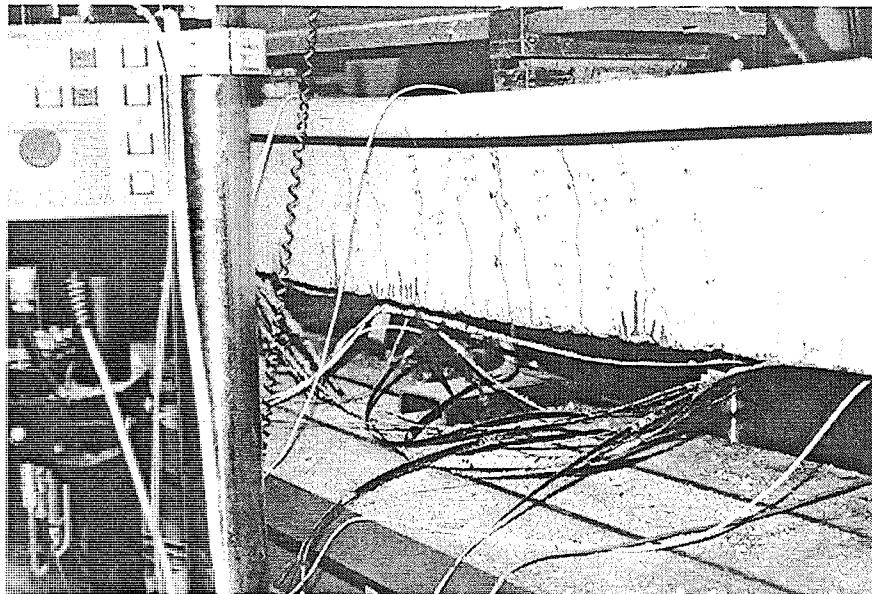


Figure 6 Tensile failure of CFRP sheet in Beam No. 2

In Beams No. 3 and No. 4 which failed by interfacial shear failure, the glued-on CFRP sheet was delaminated along the interface between the surface of concrete and CFRP sheet as shown in Figure 7. The epoxy adhesive on the CFRP sheet tore out the concrete just above the interface. The delamination seems to have started at a crack below the loading point where bending moment was maximum and suddenly propagated to the end of the CFRP sheet. Figures 8 and 9 prove that the delamination did not start from the end of the CFRP sheet, because the strains of the CFRP sheet at their ends only slightly decreased when the applied load suddenly dropped from its maximum value at onset of delamination. On the other hand, the strains in the middle of the CFRP sheet significantly decreased at onset delamination. Additional supporting evidence for this argument is that the U-shaped wrapped end anchorage in Beam No. 7 did not significantly improve the ultimate load capacity in comparison to that of Beam No. 14, which had no anchorage. When the delamination occurred on one side of the beam, the impact energy released from the tensioned CFRP sheet tore out the concrete cover already cracked vertically by flexure along the longitudinal reinforcing bars in the constant bending moment zone (Figure 7).

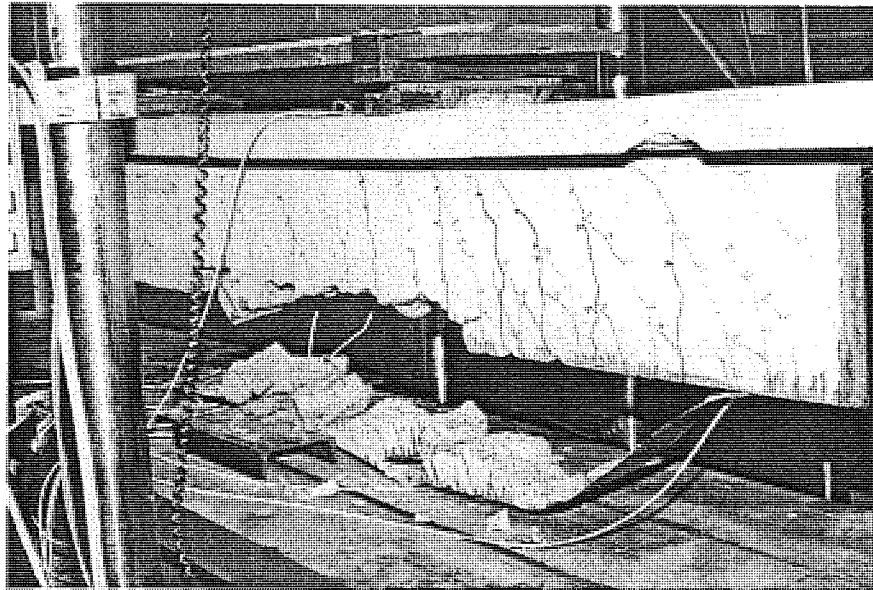


Figure 7 Interfacial shear failure of concrete in Beam No. 3.

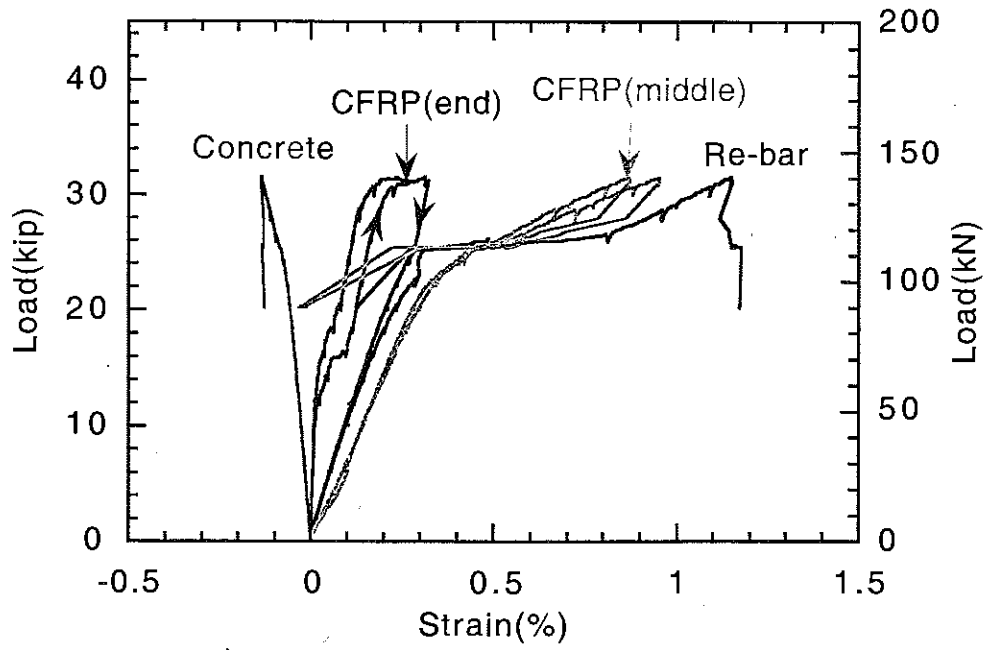


Figure 8 Load-strain curves of Beam No. 3.

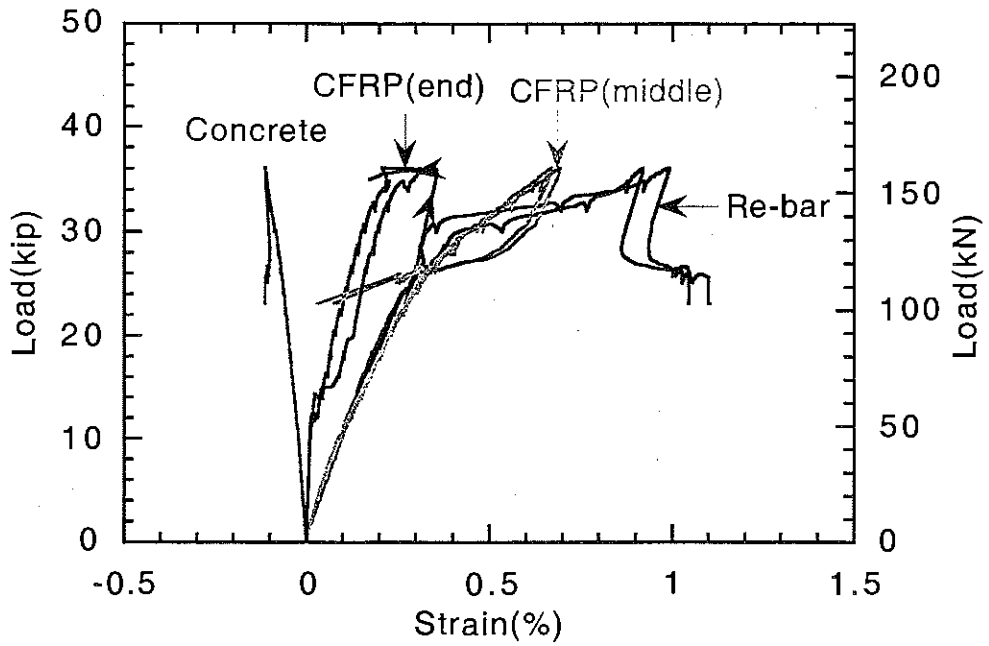


Figure 9 Load-strain curves of Beam No. 4.

Figure 10 compares the load-deflection curves of the control beam and the strengthened beams with different strengthening level (i.e., one, two, and three layers of CFRP sheets). As shown in the figure, the ultimate load considerably increased with an increase in strengthening level, while the ultimate deflection significantly decreased. Discussion about these increases in strength and decreases in deflection is covered in Section 3.1.3 Strengthening Level with the series of beams having a maximum reinforcement ratio of $0.54\rho_{max}$. The strengthened beams were stiffer than the control beam before and after reinforcement yielding. The control beam, Beam No. 1, was very ductile as expected in reinforced concrete beams with low reinforcement ratio.

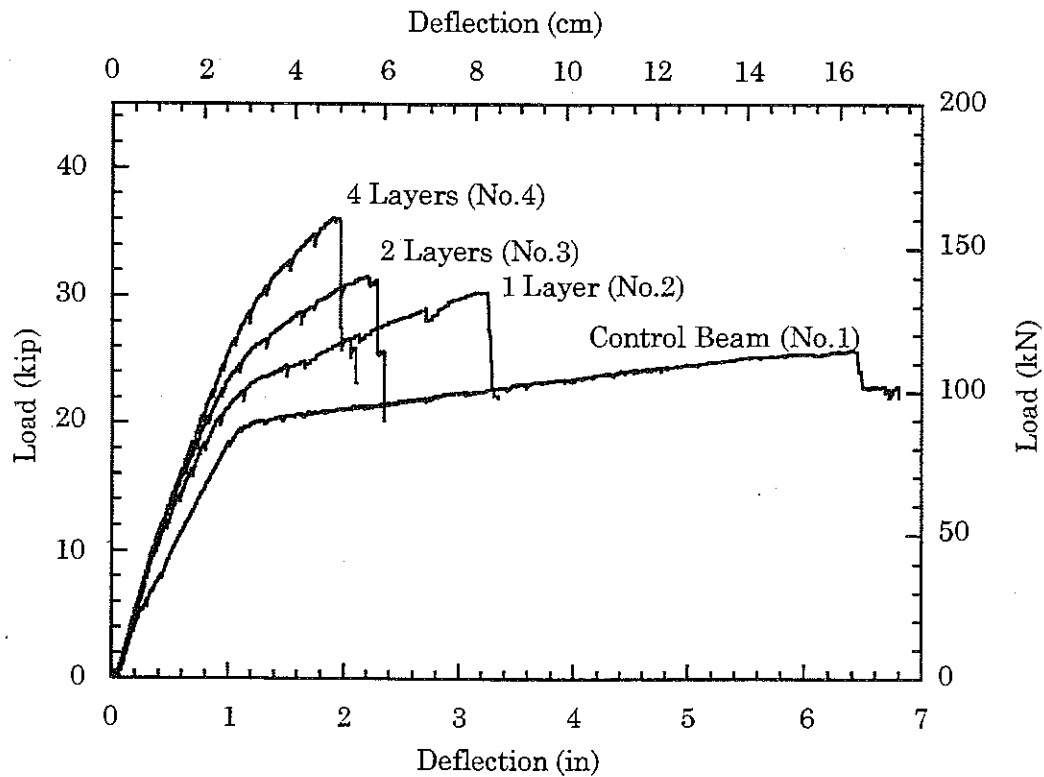


Figure 10 Load-deflection curves of beams with reinforcement ratio, $0.27\rho_{max}$, for different strengthening levels.

Figures 11 and 12 show respectively the curves for beam load and beam deflection versus the strain in the tensile reinforcing bar, at different strengthening levels. All load-strain responses of reinforcing bars were roughly bi-linear with a

yield strain of about 0.3%, which was slightly larger than the 0.24% expected yield strain. In the elastic range before yielding, the reinforcing bars in the beams strengthened using CFRP sheets had less strain. In other words, the reinforcing bars were less stressed at a given deflection. From Figure 12, it can be observed that the deflection of the control beam linearly increases as the strain of the reinforcing bar increases. However, the deflection of the beams strengthened with CFRP sheets increased linearly only prior to reinforcement yielding.

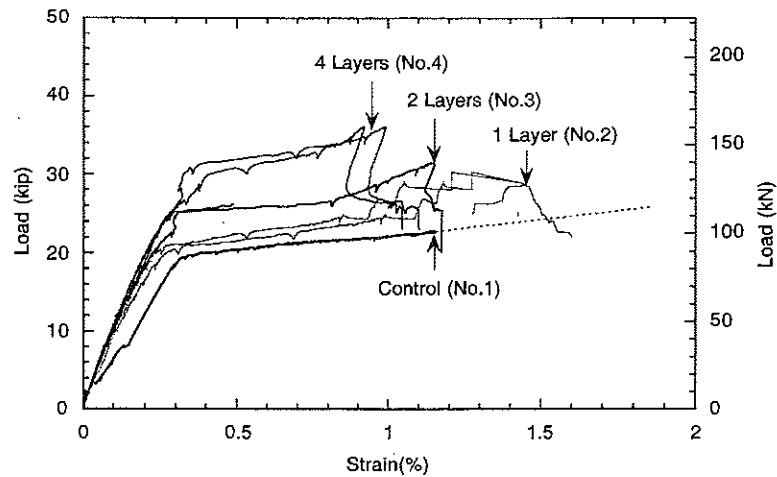


Figure 11 Load-strain curves of reinforcing bar.

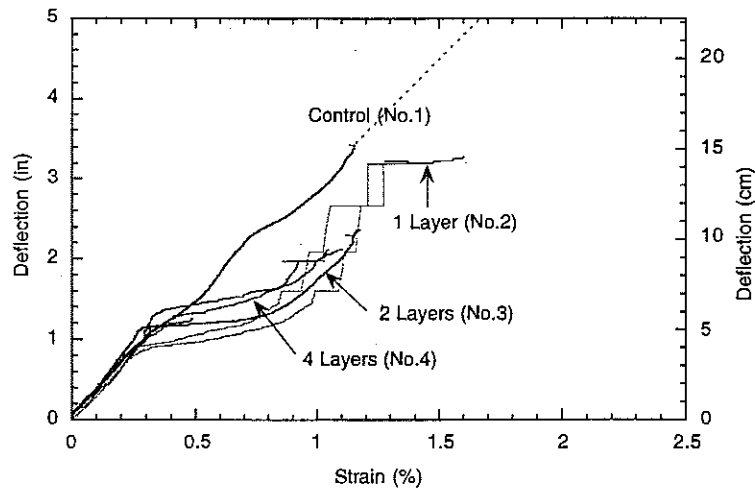


Figure 12 Deflection-strain curves of reinforcing bar.

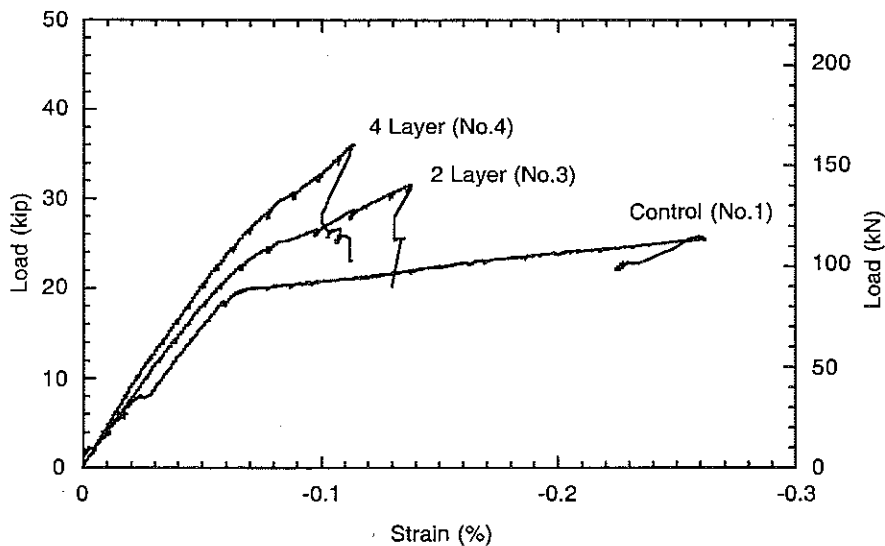


Figure 13 Load-strain curves of concrete in top flange.

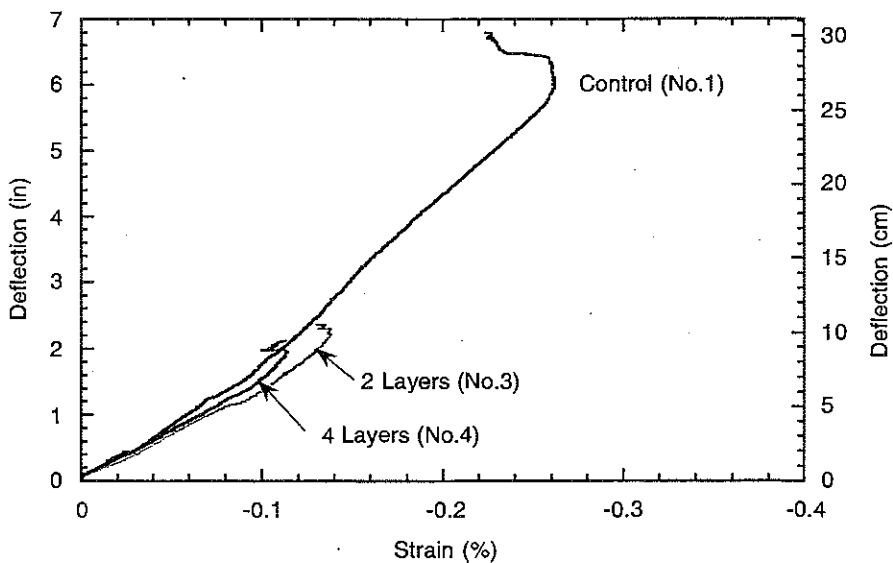


Figure 14 Deflection-strain curves of concrete in top flange.

Figures 13 and 14 show the load-strain and deflection-strain curves of the concrete top flange. Load-strain and deflection-strain curves were roughly bi-linear and linear, respectively. In the control beam, the concrete in the top flange failed by compression at a compression strain of about 0.26%. In Beam No. 3 and No. 4, the compression strains of concrete in the top flange were about 0.11 % and 0.14 % at failure by delamination of CFRP sheet, respectively. As can be seen in

Figure 13, the slope of load-strain curves increased with an increase of strengthening level. However, the deflection-strain relationship showed little difference in their slopes.

Figures 15 and 16 show the load-strain and deflection-strain curves of the CFRP glued-on sheets. As shown in Figure 15, the strain (or stress) in the CFRP sheet in Beam No. 3 and 4 was lost very rapidly following delamination of the sheet. In Beam No. 2, the CFRP sheet ruptured at about 1.45% strain, which was close to the specified failure strain of 1.5%. The deflection-strain relationship was linear up to failure with little difference in slope for different strengthening ratios. This observation implies that the strengthening effect is proportional to the strengthening level (i.e., the number of CFRP sheets). This interpretation is also confirmed by the ultimate load-strengthening level curves described in Section 3.1.3 :Strengthening Level.

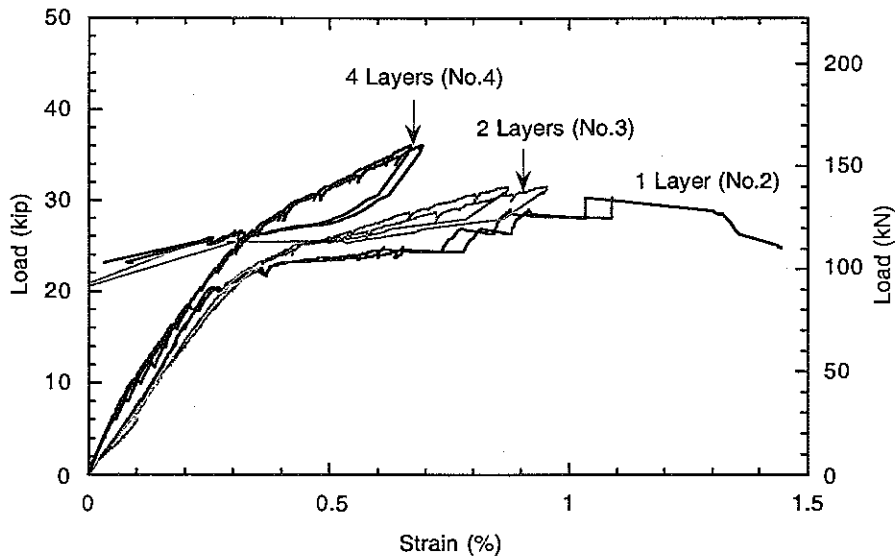


Figure 15 Load-strain curves of CFRP sheet.

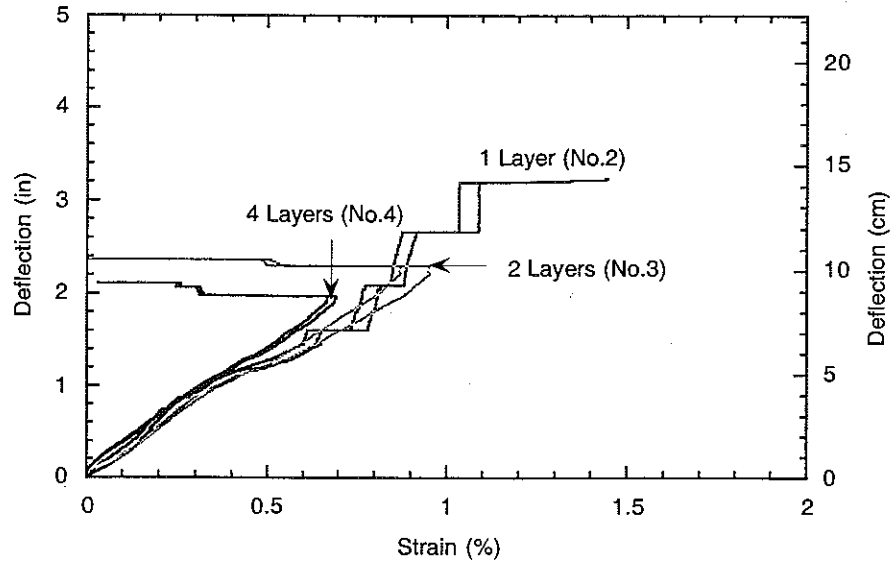


Figure 16 Deflection-strain curves of CFRP sheet.

3.1.2 Reinforcement Ratio $0.54\rho_{max}$

To study the influence of existing steel reinforcement ratio and strengthening level, the second series of beams with a maximum steel reinforcement ratio, $0.54\rho_{max}$, was tested. Beams No. 6 and No. 7 were strengthened using CFRP sheets, having a tensile strength of 3,480 MPa and a tensile modulus of 228 GPa. One layer of the CFRP sheet provided maximum tensile load of 574 N/mm width.

Upon testing, Beams No. 6 and 7 failed by interfacial shear failure of concrete (delamination) similarly to Beams No. 3 and No. 4. of the first series of tests. Control beam, Beam No. 5, failed by compression failure of the concrete in top flange after yielding of the reinforcement, as expected.

In Beam No. 6 strengthened with one layer of CFRP, only one small strip of the CFRP sheet (about one fifth of it) ruptured at the ultimate state and, shortly thereafter, the remaining part of the CFRP sheet delaminated with only two pieces of concrete spalled off from the concrete cover as shown in Figure 17. This combination of tensile rupture and delamination of CFRP sheet indicates that the CFRP sheet almost reached its failure stress (or strain) in tension, implying that it was fully effective in terms of strengthening. This conclusion was confirmed later

from analysis of the load-strain curves of CFRP sheet. The measured strain at the ultimate load was about 1.4%, which is slightly less than the specified strain of 1.5% (Figure 21).

Figure 18 compares the load-deflection response curves of the control beam and the beams strengthened with one and two layers of CFRP sheets. Figures 19 to 22 show the corresponding load-strain and deflection-strain curves of the reinforcing bar and the CFRP sheets. The analysis of these results is very similar to that carried out for the beams with a maximum steel reinforcement ratio, $0.27\rho_{max}$, even though their numerical values are different.

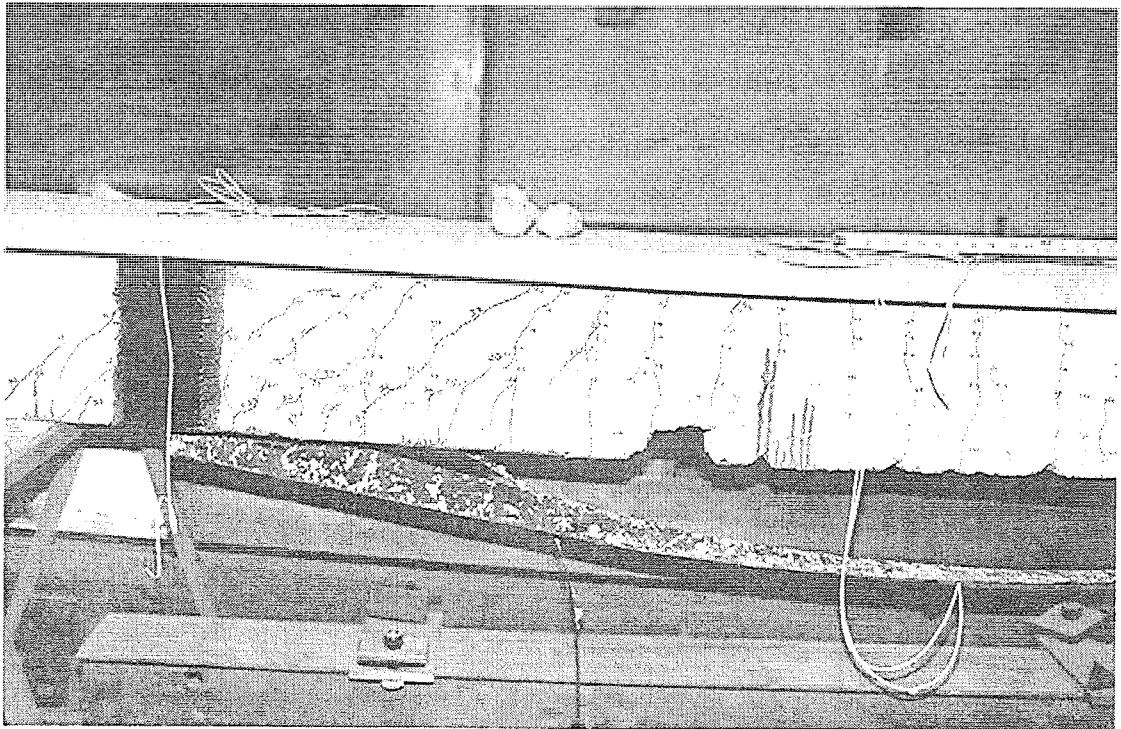


Figure 17 Tensile rupture and delamination of CFRP sheet in Beam No. 6.

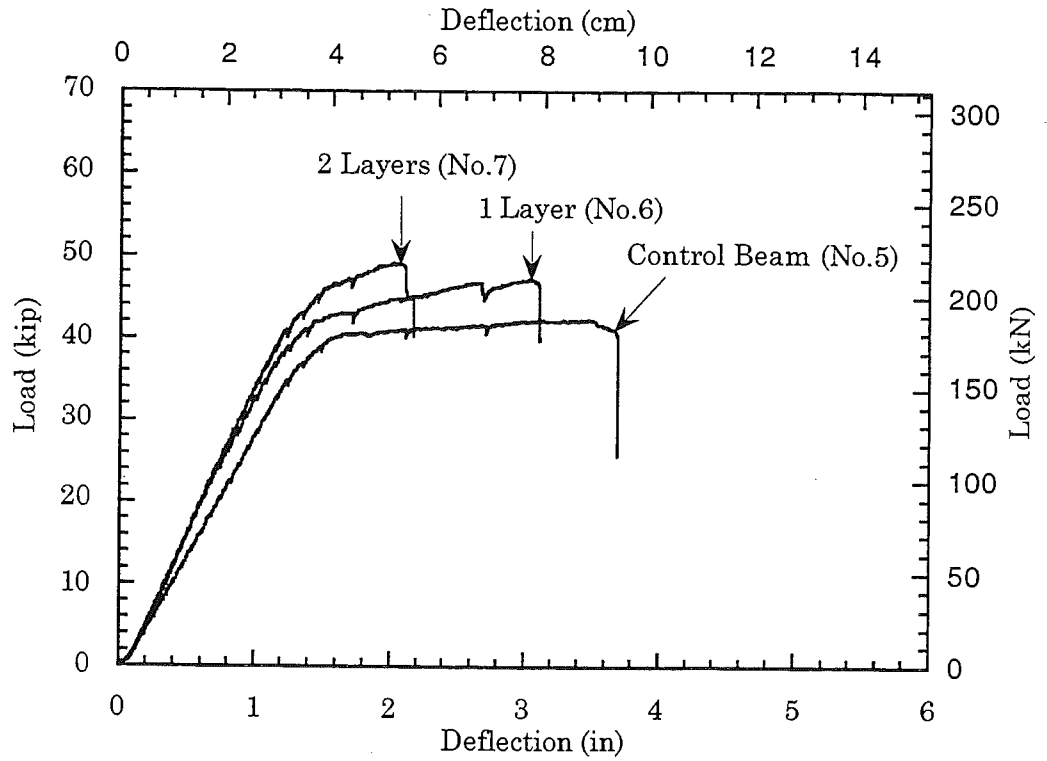


Figure 18 Load-deflection curves of beams with reinforcement ratio, $0.54\rho_{max}$, at two strengthening levels.

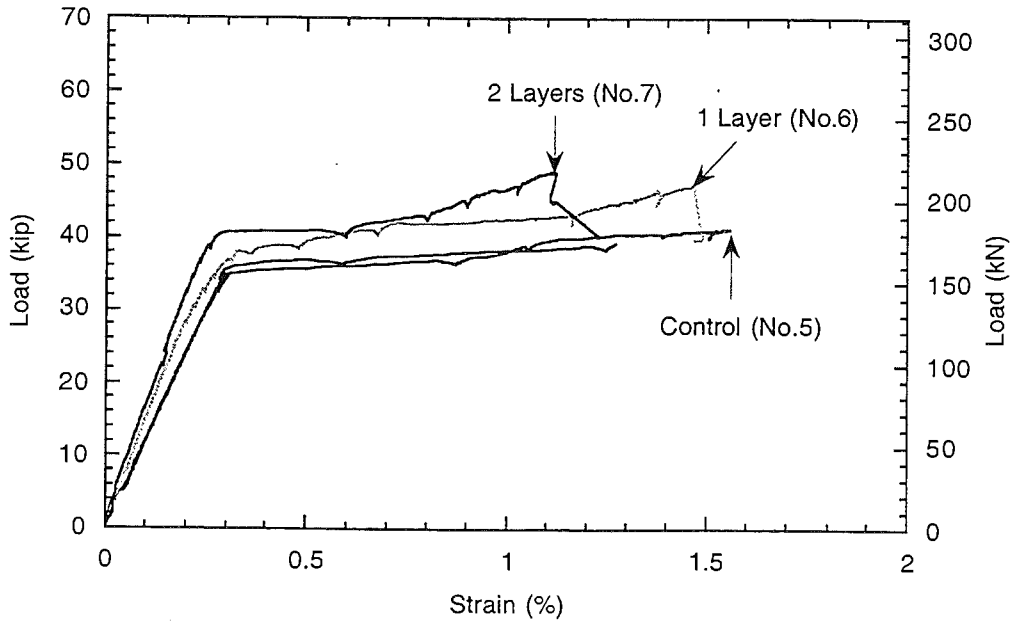


Figure 19 Load-strain of reinforcing bar of beams with reinforcement ratio, $0.54\rho_{max}$, at two strengthening levels.

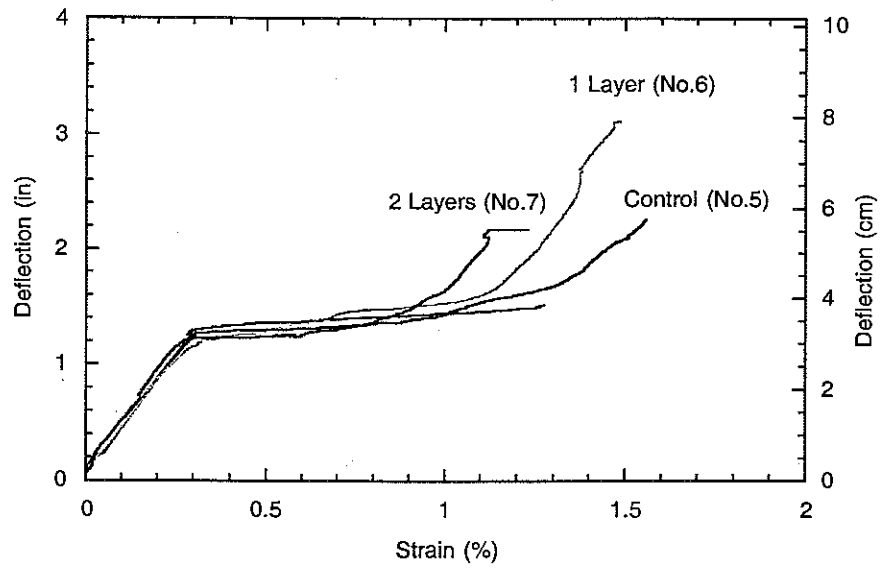


Figure 20 Deflection-strain curves of reinforcing bar of beams with reinforcement ratio, $0.54\rho_{max}$, at two strengthening levels.

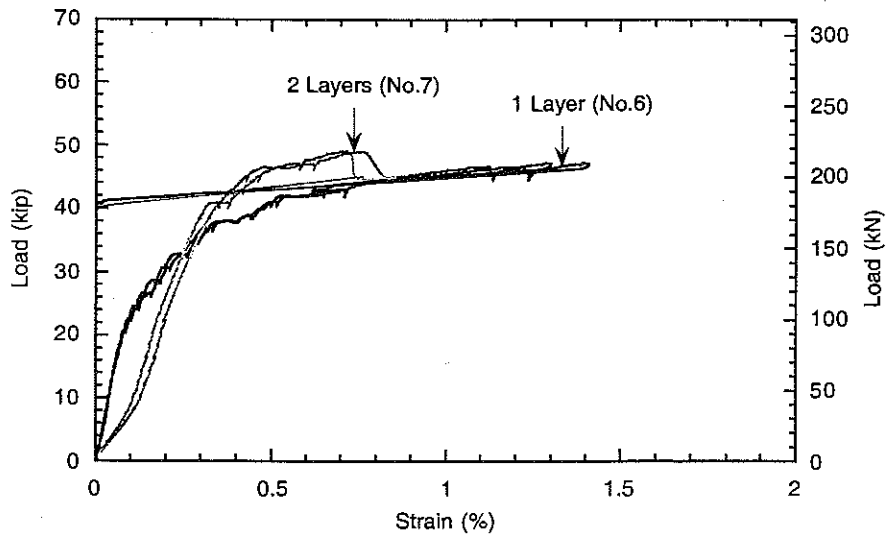


Figure 21 Load-strain curves of CFRP sheet of beams with reinforcement ratio, $0.54\rho_{max}$, at two strengthening levels.

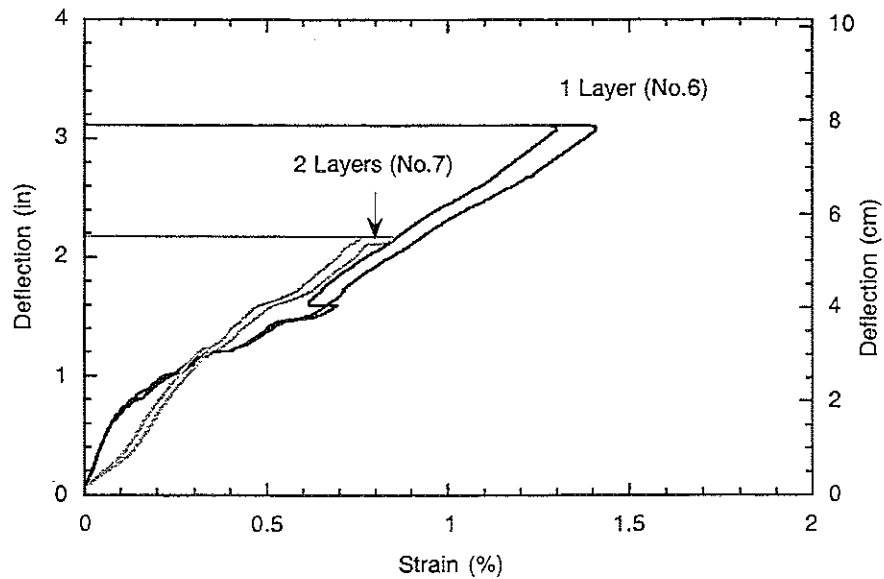


Figure 22 Deflection-strain curves of FRP sheet of beams with reinforcement ratio, $0.54\rho_{max}$, at two strengthening levels.

3.1.3 Influence of Strengthening Level

In the experimental study of the parameters, steel reinforcement ratio and strengthening level, several findings were observed. Some numerical results are given in Table 7.

1. For a given reinforcement ratio, the ultimate load capacity increases with the strengthening level, or the number of CFRP sheets (Figure 23).
2. The increment in ultimate load increase obtained by strengthening was almost proportional to the strengthening level or number of CFRP sheets (Figure 24). However, this direct relationship should be further confirmed experimentally in beams with higher strengthening levels and higher reinforcement ratios.
3. The almost equal slopes of the two lines shown in Figure 24 suggest that the increment of ultimate load achieved by strengthening is not significantly affected by the reinforcement ratio. However, the lower the reinforcement ratio, the higher the strengthening effect in terms of percent increase in ultimate load capacity (Figure 25).

4. The ultimate deflection of strengthened beams decreased as the strengthening level increased (Figure 26), that is a lower ductility is obtained. This is one of the disadvantages of beams strengthened using CFRP sheets. However, the strengthened beams had, after failure or delamination of the CFRP sheets, a minimum loading capacity and ductility which were almost same as those of the control beam, in spite of the fact that the concrete cover in the constant moment zone was severely damaged (see Section 3.7 Residual Strength of Beam after Failure).
5. The total tensile force contributed by the CFRP sheets at failure, increased linearly with the strengthening level (or number of sheets used) (Figure 27).

In Figure 27, the total tensile force was calculated from the following equation:

$$T = \Delta M / (h - h_f/2)$$

where ΔM is the difference in moment capacity (observed experimentally) between the strengthened beam and the control beam, taken at the failure deflection of the strengthened beam, h is the total depth of the beam and h_f is the depth of the flange of the T section used. Note that $(h - h_f/2)$ represents, as a first approximation, the lever arm from the centroid of the strengthening sheets to the centroid of the compression force in the concrete. In Figure 27, a value of calculated T is also shown; it is based on equilibrium and strain compatibility of the section at the observed ultimate load of the beam. The two values are comparable and provide some confidence in the calculations.

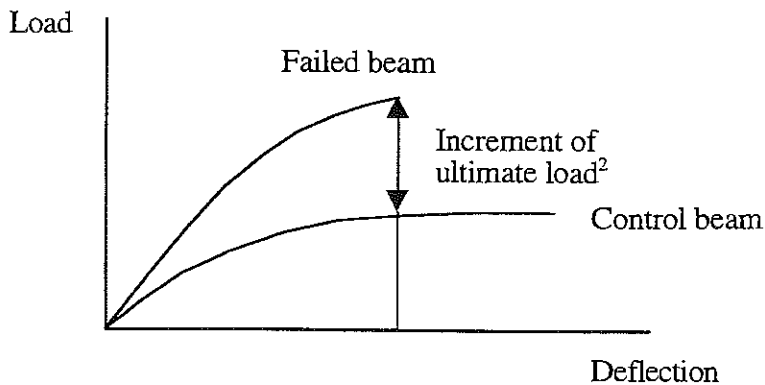
Table 7 Summary of test results of Beams with different strengthening levels.

Beam No.	1	2	3	4	5	6	7
Reinforcement ratio	$0.27\rho_{max}$	$0.27\rho_{max}$	$0.27\rho_{max}$	$0.27\rho_{max}$	$0.54\rho_{max}$	$0.54\rho_{max}$	$0.54\rho_{max}$
No. of CFRP sheet layer	0	1	2	4	0	1	2
Type of failure ¹	S.Y	T.F.	I.S.F	I.S.F	S.Y	I.S.F	I.S.F
Ultimate load, kN	114.8	135.0	140.4	160.7	188.0	209.9	222.0
Ultimate deflection, mm	16.4	8.3	5.6	4.9	8.8	7.7	5.2
Yielding load, kN	89	102	116	133	180	191	207
Increment of ultimate load, kN	0	20.2	25.6	45.9	0	21.9	34.0
Increment of yielding load, kN	0	13.3	26.7	44.5	0	11.1	26.7
Increment of ultimate load ² , kN	0	34.7	44.9	66.3	0	23.1	36.5
Measured CFRP tensile stress, MPa	-	3285	2074	1544	-	3049	1654
Measured CFRP tensile force, kN	-	55.2	69.4	103.6	-	40.9	55.6
Calculated CFRP tensile force, kN	-	56.9	73.4	108.5	-	37.8	59.6
Measured shear stress of concrete (MPa)	-	0.76	0.96	1.43	-	0.57	0.80
Calculated shear stress of concrete (MPa)	-	0.79	1.02	1.50	-	0.52	0.82

1: S.Y: Steel Yielding; T.F. = Tensile failure of CFRP sheet

I.S.F: Interfacial Shear Failure of concrete (delamination failure)

2: Increment of the ultimate load at the same deflection of failed beam, see sketch below.



6. It seems that the contribution of the shear resistance of concrete to the strength of the interface, linearly increases with the strengthening level (Figure 28). In Figure 28, the interface shear stress of concrete was calculated based on the assumption of equal shear stress along the shear span.

The shear stress at the interface between the CFRP sheets and the concrete at failure of the beam (by delamination) was calculated from the tensile force T (described above in 5.) assuming horizontal shear stresses are equally distributed over the shear span. This leads to the equation:

$$\tau = T / (WL_a)$$

Where W is the width of the CFRP sheet or contact area, and L_a is the distance from the loading point (maximum moment point) to the end of the CFRP sheet. Here also the second value of shear "calculated" and shown in Figure 28 corresponds to the value of T obtained from analysis of the section at ultimate moment capacity as described in 5.

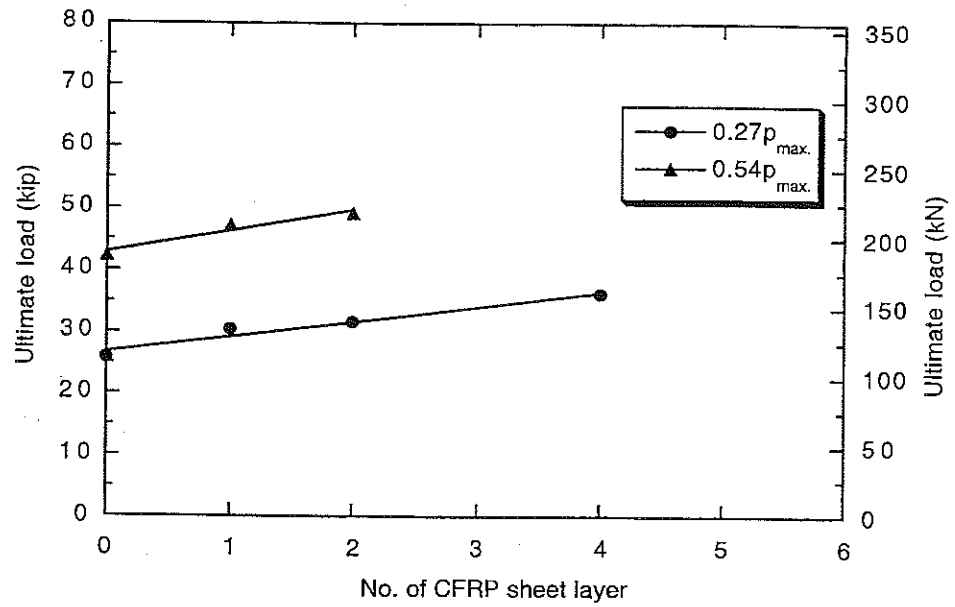


Figure 23 Relationship between ultimate load and strengthening level.

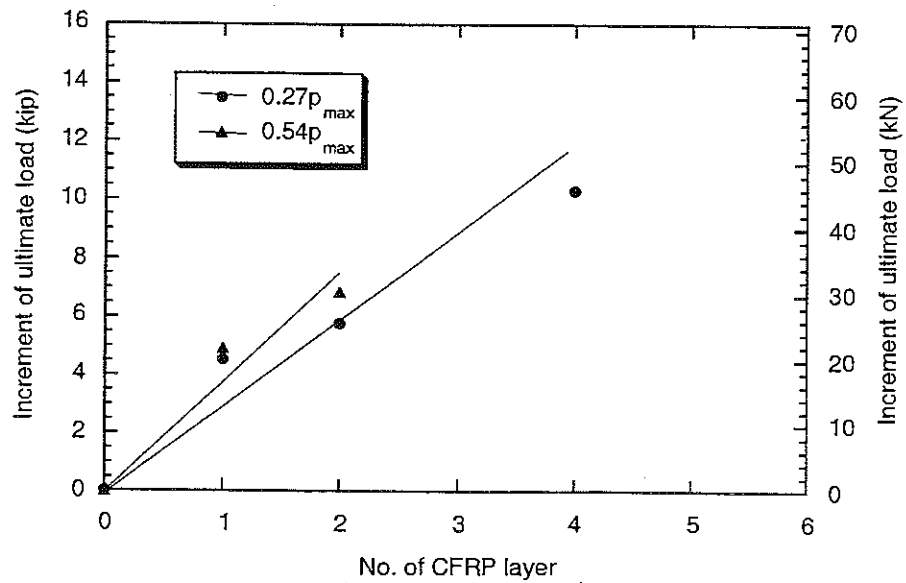


Figure 24 Increment of ultimate load versus strengthening level.

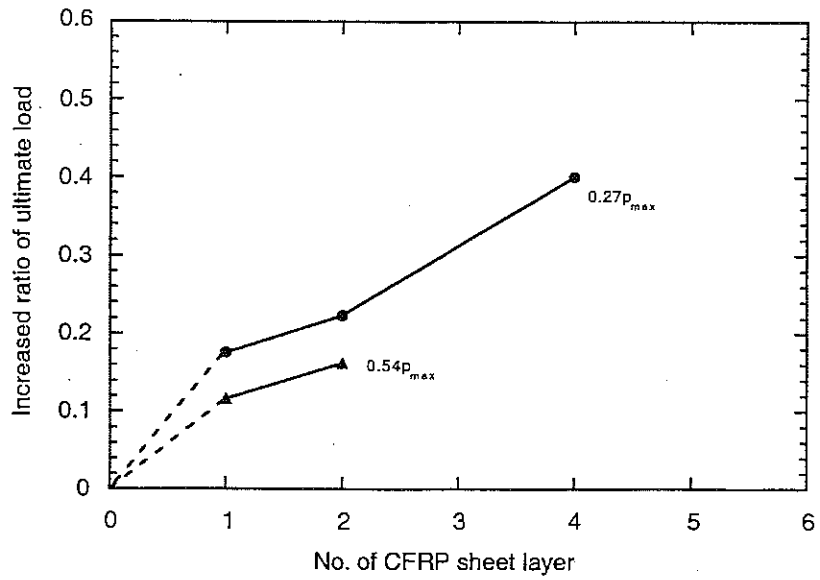


Figure 25 Increase in ratio of ultimate load versus strengthening level.

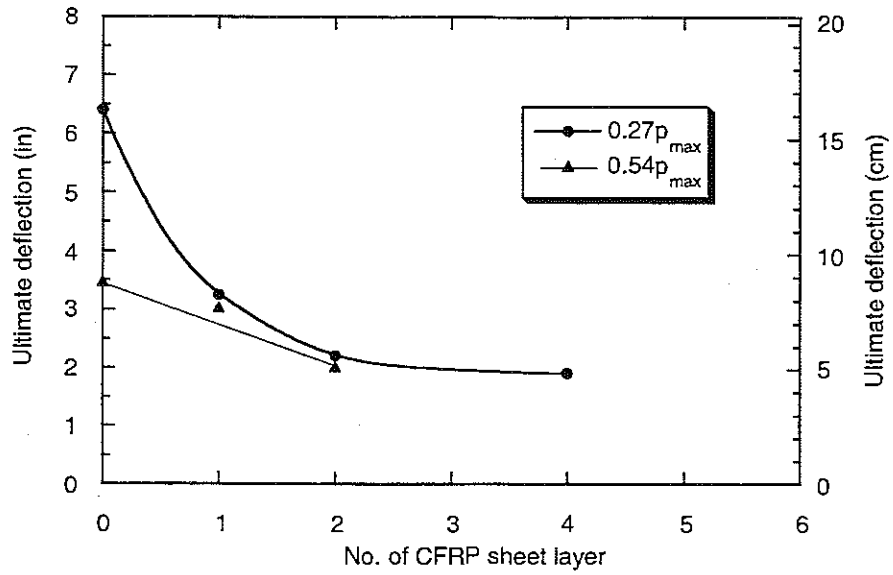


Figure 26 Ultimate deflection versus strengthening level.

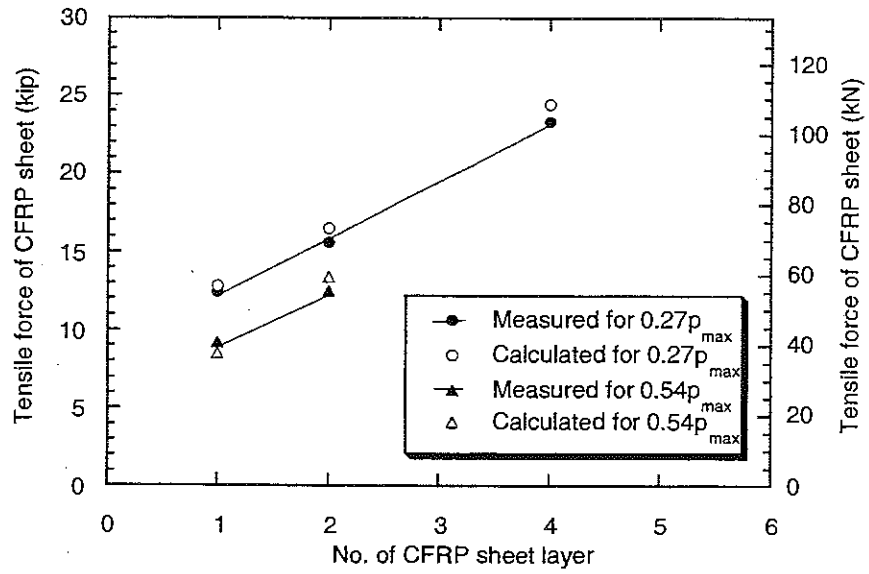


Figure 27 Tensile force of CFRP sheet versus strengthening level.

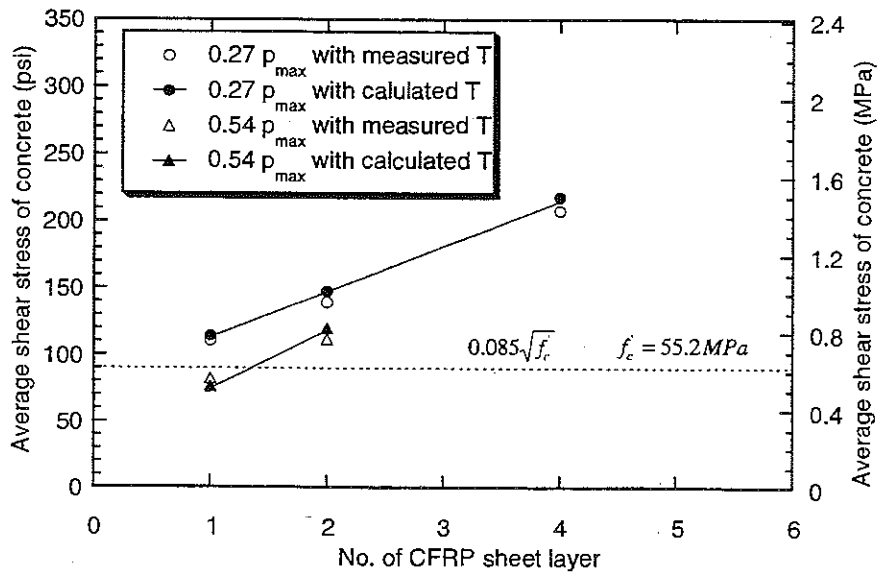


Figure 28 Shear stress of concrete at delamination of CFRP sheet.

3.2 Influence of Strengthening System

To compare the two strengthening systems tested, the results of Beams No. 8 and No. 8-1 are compared with those of Beam No. 7. Beams No. 8 and No. 8-1 were strengthened using CarboDur (Sika) CFRP plate having a tensile strength of 2,400 MPa and a tensile modulus of 150 GPa, while Beam No. 7 was strengthened with Forca Tow sheet (Tonen), having a tensile strength of 3,480 MPa and a tensile modulus of 228 GPa. One layer of Sika CFRP plate and Tonen CFRP sheet, 100 mm wide, provided a tensile strength of 2,868 N/mm width and 574 N/mm width, respectively. The 40 mm wide Sika CFRP plate used in Beam No. 8 was equivalent to two layers of 100 mm wide Tonen CFRP sheets in terms of failure strength.

All three beams failed by interfacial shear failure in the concrete (delamination) just above the epoxy adhesive. Unlike Beam No.7, Beam No. 8 had no pieces of concrete cover spalled off (Figure 29). This fact can be attributed to the smaller bond width of 40 mm of the Sika plate. Beam No. 8 was in very good shape even after delamination of the CFRP plate, and was later re-used as Beam No. 8-1 strengthened with 100 mm wide Sika plate thus the strengthening level of Beam No. 8-1 was about 2.5 times that of Beam No. 8. Upon testing, Beam No. 8-1 was severely damaged by the delamination failure as shown in Figure 30, where large chunks of concrete cover spalled off.

Figure 31 compares the load-deflection curves of the three strengthened beams, using Sika and Tonen systems, with the control beam. It can be observed that the load-deflection response of Beam No. 8 using the Sika system was almost the same as Beam No. 7 with the Tonen system; the difference in the tensile modulus of the two systems (the modulus of Sika CFRP plate was about two thirds that of Tonen CFRP sheet) had little influence on the elastic portion of the curve. The ultimate load and deflection of the beam with the Sika system were respectively about 4% and 11% less than those of the beam with the Tonen system. Beam No. 8-1 with the 100 mm Sika plate showed a very stiff load-deflection response because of its high strengthening level. The ultimate strength of Beam No. 8-1 was higher while its ultimate deflection was smaller than those of Beams No.7 and No. 8 (Figure 31).

Figures 32 to 37 show the load-strain and deflection-strain curves of respectively the reinforcing bar, concrete in top flange, and the CFRP laminate at the mid span section. These figures are provided as additional information. For instance, it can be observed that the strain in the Sika CFRP plate in Beam No. 8

was almost the same as that of the Tonen CFRP sheet in Beam No. 7 (Figures 36 and 37).

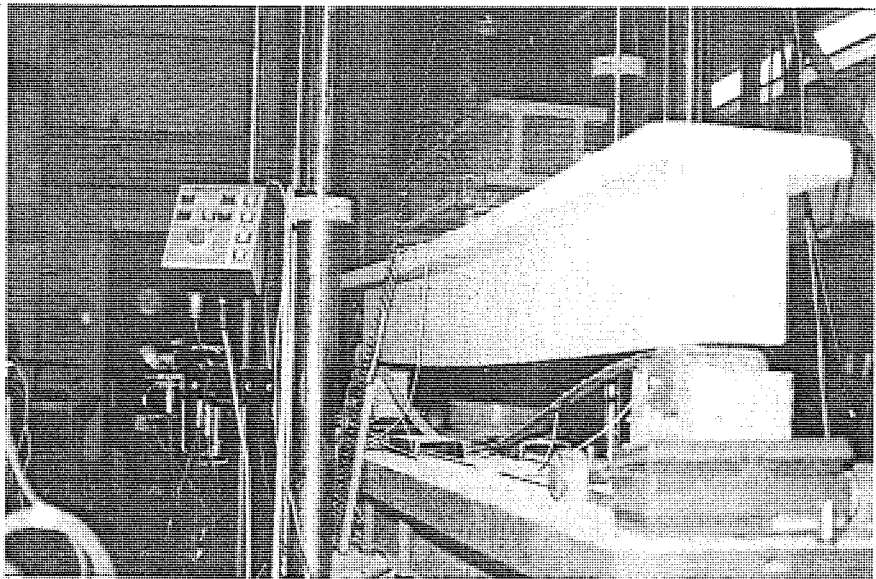


Figure 29 Interfacial shear failure (delamination) of concrete in Beam No.8

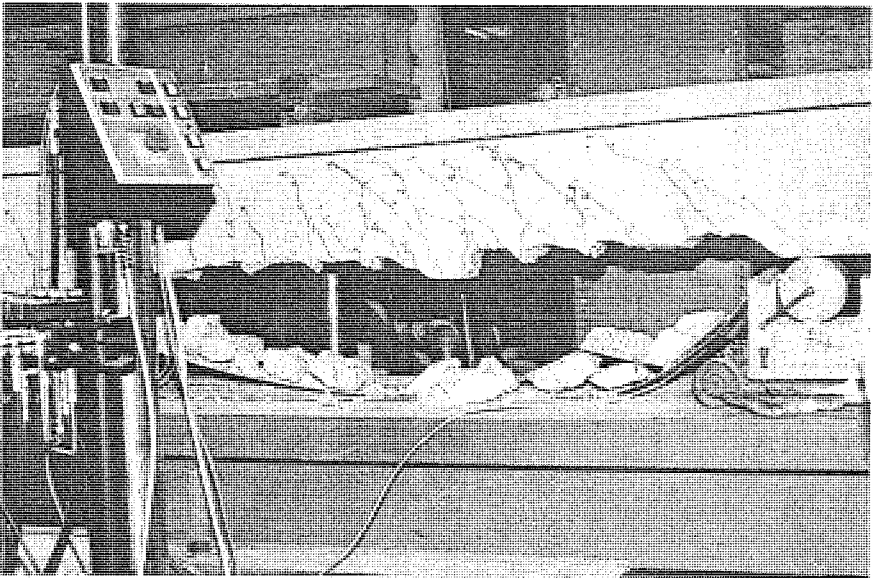


Figure 30 Interfacial shear failure of concrete in Beam No.8-1

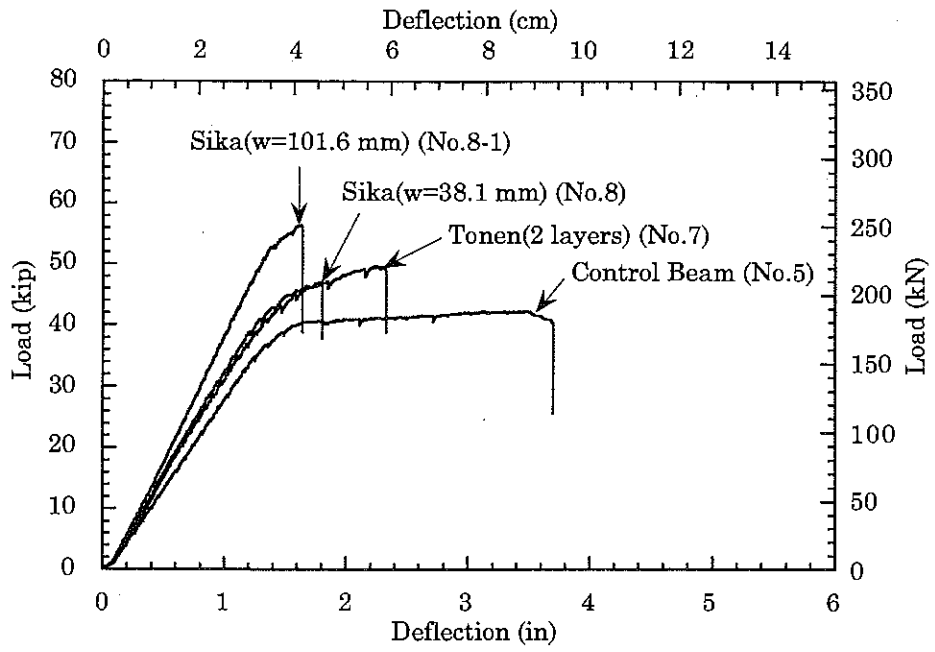


Figure 31 Load-deflection curves for different strengthening systems.

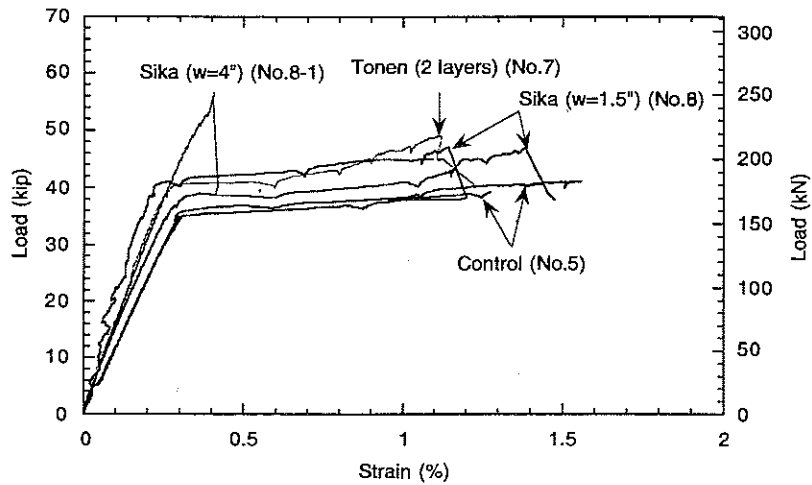


Figure 32 Load-strain curves of reinforcing bar.

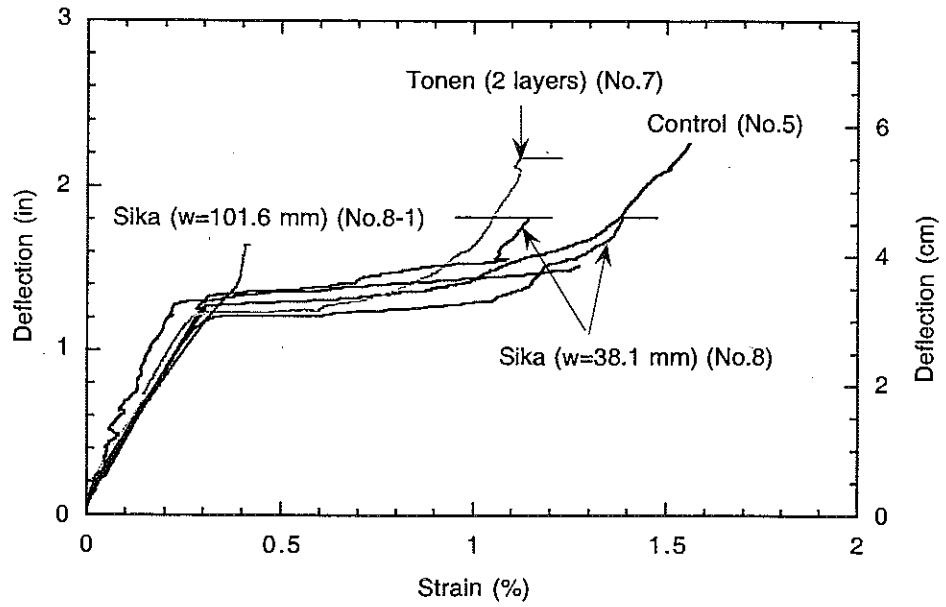


Figure 33 Deflection-strain curves of reinforcing bar.

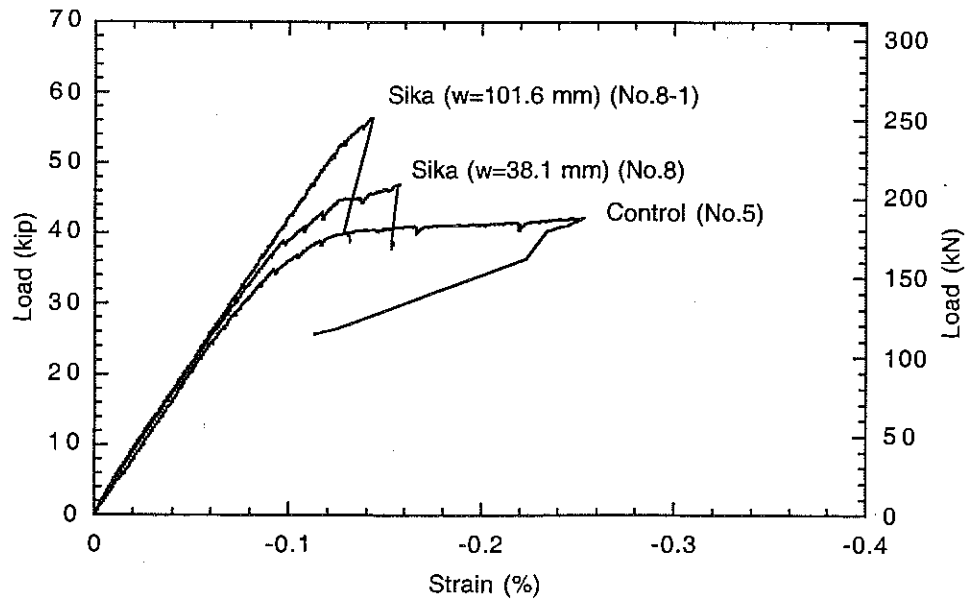


Figure 34 Load-strain curves of concrete.

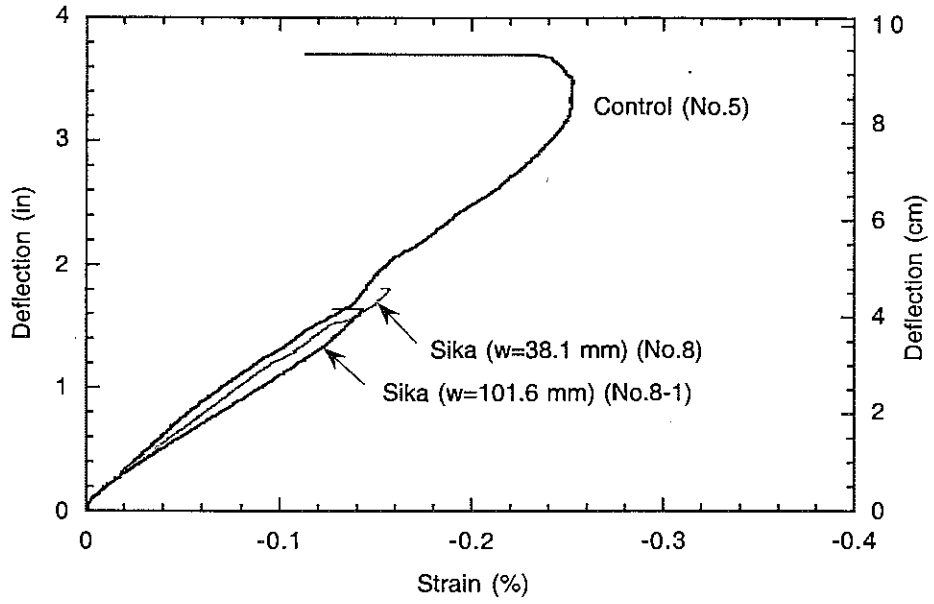


Figure 35 Deflection-strain curves of concrete.

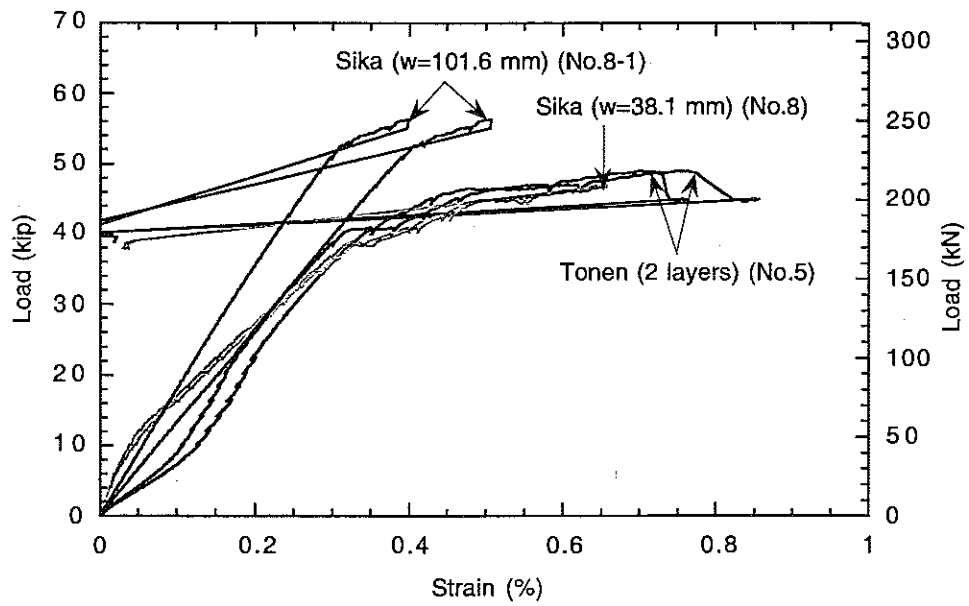


Figure 36 Load-strain curves of CFRP sheet.

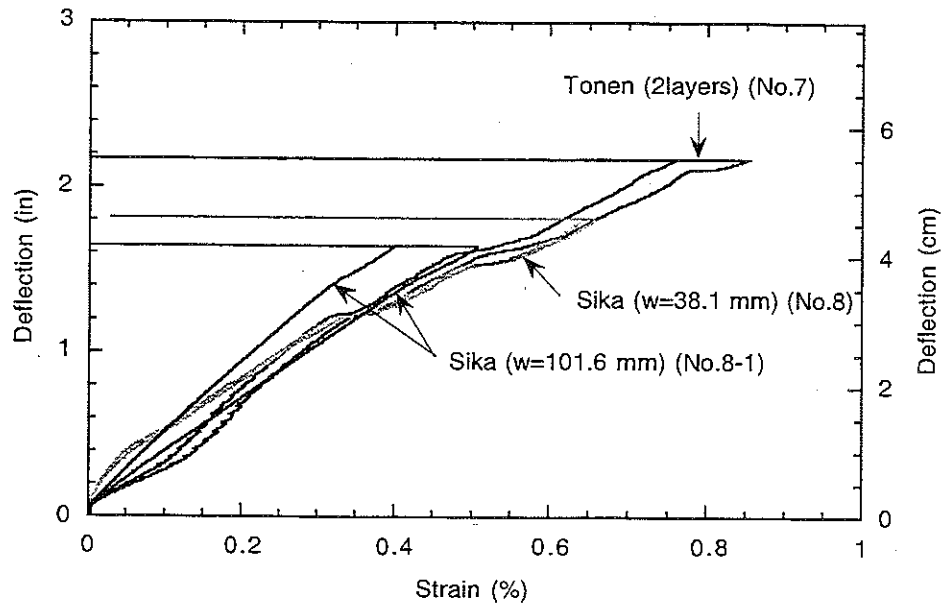


Figure 37 Deflection-strain curves of CFRP sheet.

3.3 Influence of Concrete Cover

To investigate the effect of concrete cover, Beams No. 12 and No. 9 were tested and compared to Beam No. 7. Beams No. 12 and No. 7 had 25 mm and 50 mm net concrete cover depth, respectively. Beam No. 9 had 25 mm existing concrete cover as cast, and 25 mm additional cover added with epoxy mortar to simulate a repair. All beams had the same effective depth from the top concrete fiber to the longitudinal steel reinforcement and the same reinforcement ratio, $.54\rho_{max}$.

Beam No. 12 with 25 mm deep cover and Beam No. 7 with 50 mm deep cover failed by interfacial shear failure of concrete (delamination). Beam No. 9 with repaired concrete cover, failed by interfacial bond failure between the repair mortar and the existing concrete (Figure 38)

The load-deflection curves of the three beams are compared in Figure 39. Surprisingly, it is observed that the concrete cover considerably affected the ultimate deflection of the strengthened beam. Beam No. 12 with 25 mm cover had

about 35% larger ultimate deflection than Beam No. 7 with 50 mm cover. Yet they both had about the same strength.

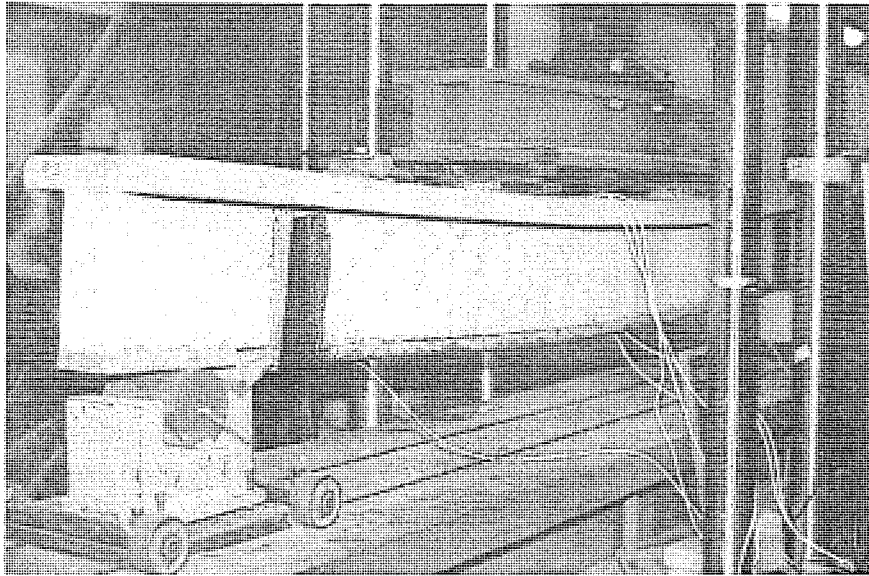


Figure 38 Interfacial bond failure of CFRP sheet in Beam No. 9.

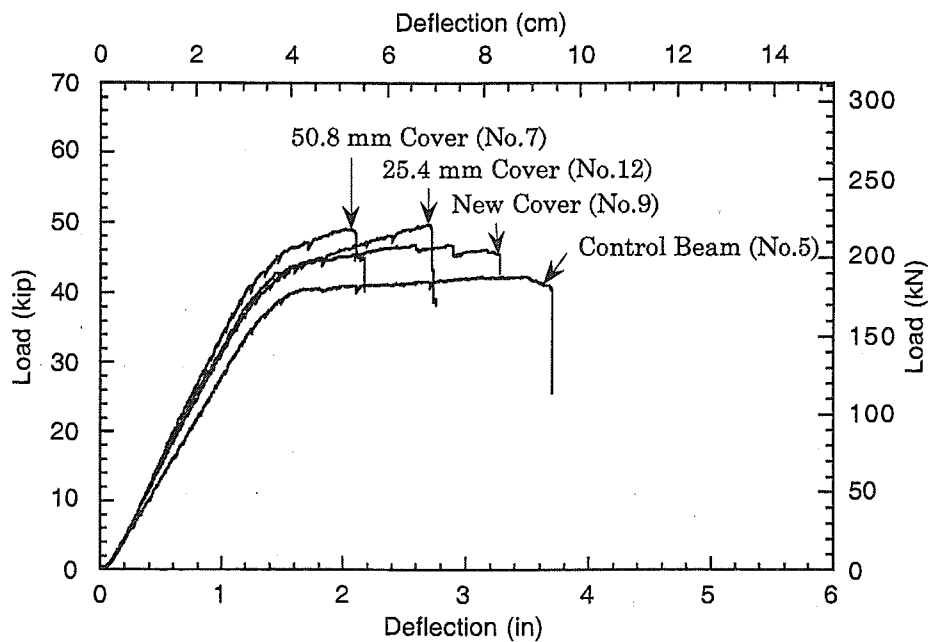


Figure 39 Load-deflection curves of beams with different concrete cover.

Compared to Beams No. 7 and 12, Beam No. 9 showed a more ductile behavior. Its ultimate deflection, 83 mm, was about 60% larger than that of Beam No. 7. The reason for this increase is believed to be due to the gradual debonding of the interface between the repair mortar and existing concrete. However, the increase in load due to strengthening, 20.2 kN, was about 35% less than that of Beam No. 7.

3.4 Influence of End Anchorage

To evaluate the effect of different anchorage systems, Beams No. 10 and No. 14 were tested and compared with Beam No. 7. For Beam No. 10, CFRP sheet was extended and glued up to the support without having a wrapped end U-shaped anchorage. Beam No. 14 had neither a wrapped end anchorage nor an extended end anchorage. Beam No. 7 had a 100 mm wide wrapped end anchorage.

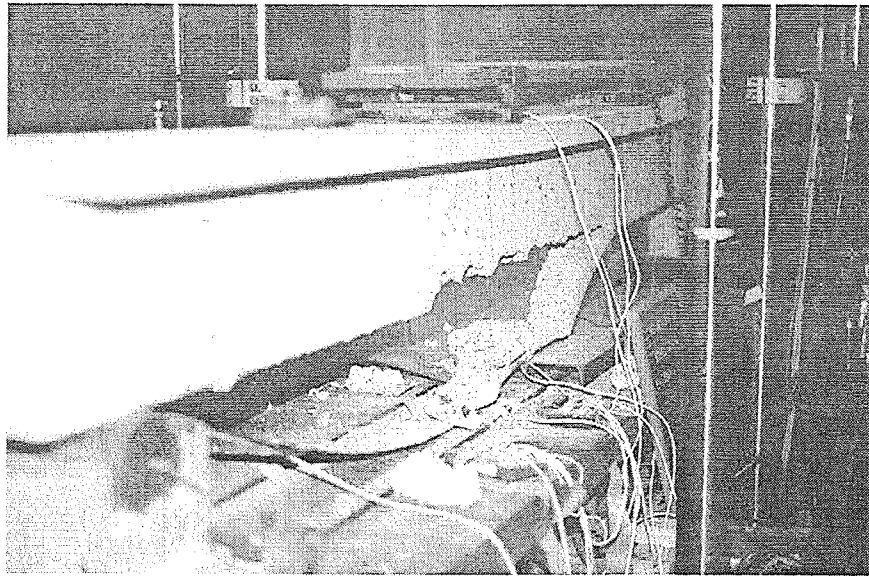


Figure 40 Interfacial shear failure of concrete in Beam No. 10.

All three beams failed by interfacial shear failure of concrete (delamination) regardless of their type of anchorage. In all three beams, delamination damaged the concrete cover in the constant moment zone (Figures 40 and 41). Beam No. 14 had one piece of concrete cover torn off at the end of the CFRP sheet.

The load-deflection curves of the three beams are compared in Figure 42. For all practical purposes, all three beams had the same ultimate load and the same ultimate deflection, regardless of their anchorage system.

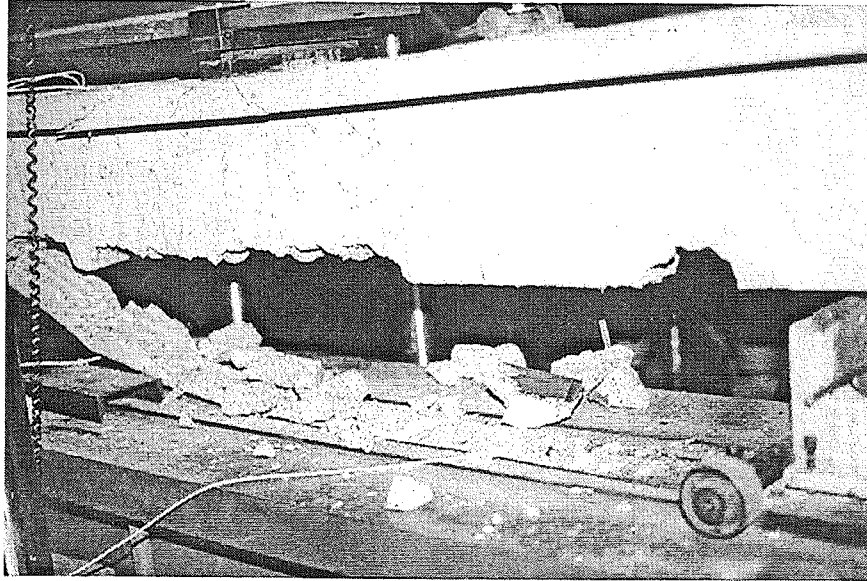


Figure 41 Interfacial shear failure of concrete in Beam No. 14.

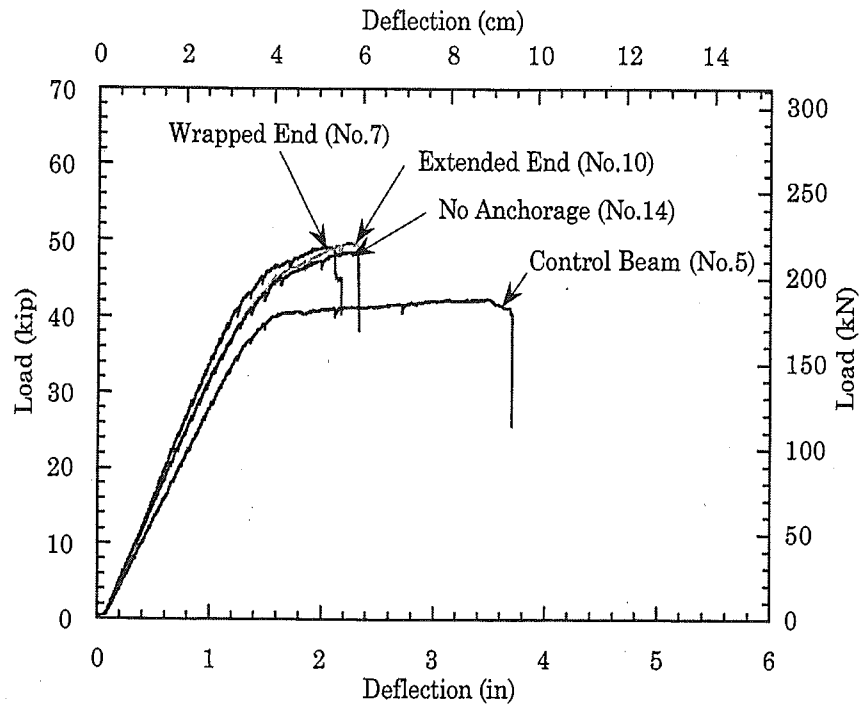


Figure 42 Load-deflection curves of beams with different anchorage.

This may suggest that in spite of stress concentration effects at the ends of the glued-on sheets, the failure crack may have started elsewhere along the beam, very likely at the site of an existing flexural crack, near the point of maximum load. So improving the end anchorage beyond what is strictly needed as development length, does not seem necessary.

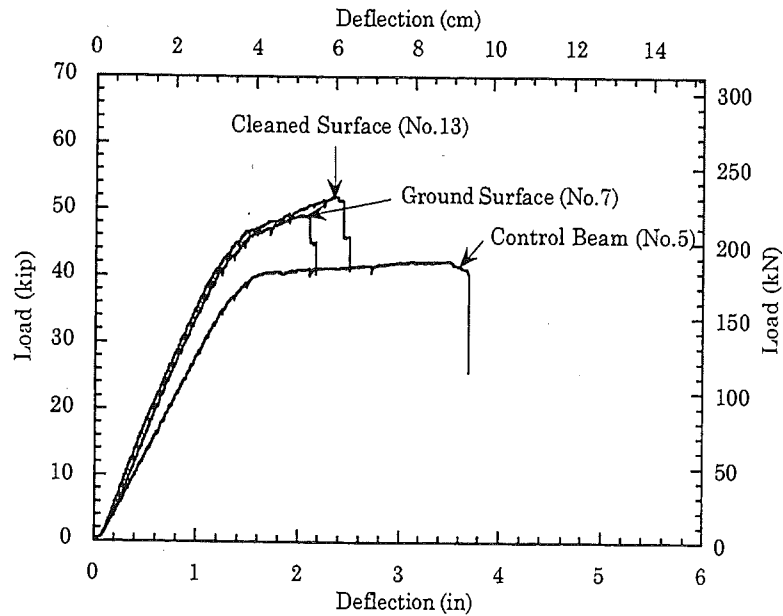


Figure 43 Load-deflection curves of beams with different surface preparation.

3.5 Influence of Surface Preparation

To evaluate the importance of surface preparation, Beam No. 13 was prepared without grinding the surface of concrete to be glued-on. The concrete surface was simply vacuum cleaned and wiped off with clean cloth. The load-deflection response curve of Beam No. 13 is compared in Figure 43 with that of Beam No. 7 which was prepared with a ground surface. No notable difference can be observed. Both beams failed by interfacial shear failure of the concrete (delamination). In fact, Beam No. 13 without ground surface, showed a slightly higher strength and deflection. This test result may imply that a well cleaned surface of concrete is enough to develop a good bond strength with epoxy adhesive. However, this conclusion should be experimentally confirmed by additional tests, because the concrete used in this test was new, and its surface was not subjected to any prior environmental deterioration.

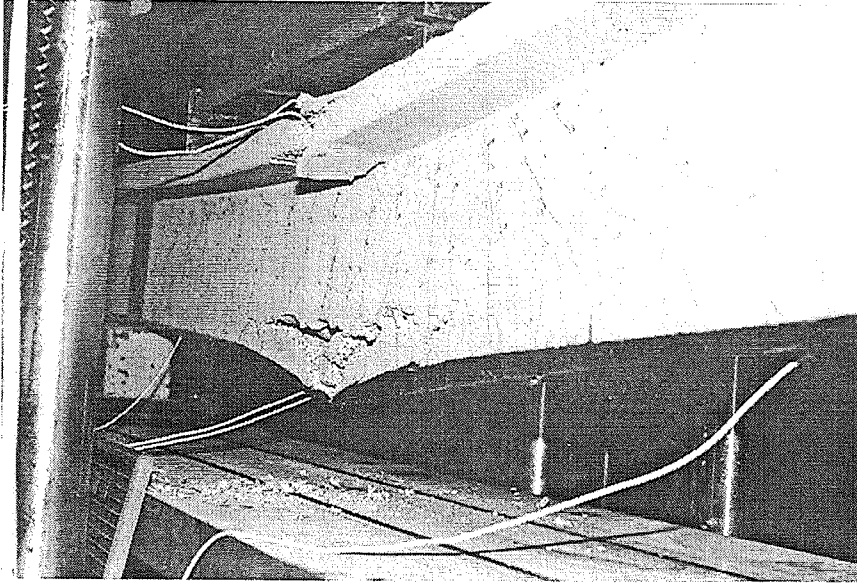


Figure 44 Inter-laminar shear failure of Beam No. 11.

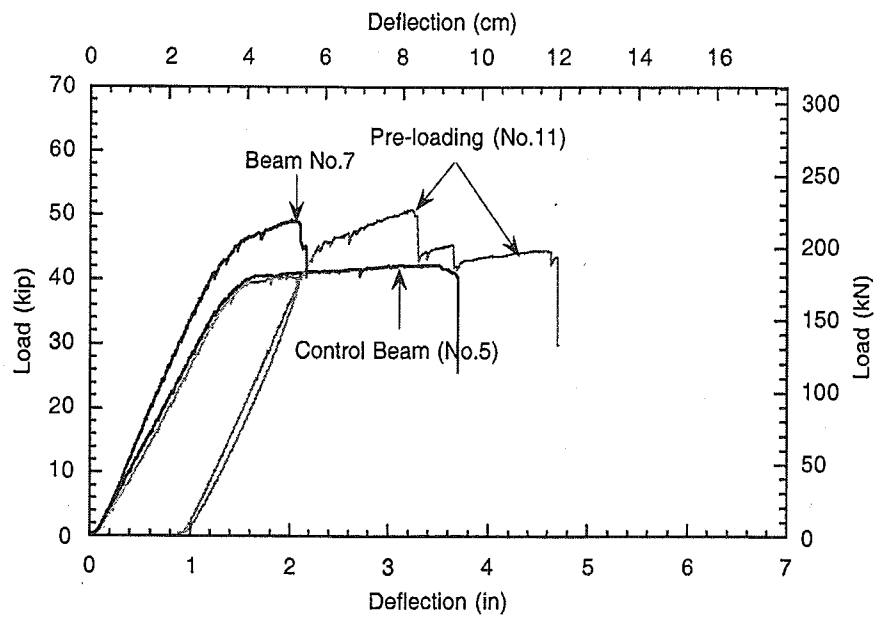


Figure 45 Load-deflection curves of beams with different loading history.

3.6 Influence of Loading History

To investigate the effect of loading history, before the application of CFRP sheets, on the flexural behavior of strengthened beams, Beam No. 11 was pre-loaded to about 180 kN, a load clearly beyond the yielding of the steel reinforcing bars (Figures. 44 and 45). The permanent deflection and maximum crack width in the pre-cracked beam at unloading, were about 24 mm and 0.9 mm, respectively. After unloading, two layers of Tonen CFRP sheets were glued to the beam, following exactly the same procedure as for previous beams. The reason for pre-loading and pre-cracking was to simulate a severely damaged beam in real situation.

Unlike other beams, the pre-loaded beam, Beam No. 11 failed by inter-laminar shear failure within the first layer of the glued on CFRP sheet (Figure 44). This failure mode is thought to be due to the imperfect penetration of epoxy into the fibers of the first layer, and is independent of the pre-loading condition. At the time of gluing the CFRP sheet, the epoxy resin was six-month old (after the bucket was first opened). The resin was quite thick and very difficult to mix because of hardened lumps and high viscosity. However, in spite of that, the ultimate load of Beam No. 11 was about the same as that of Beam No.7. Also, its concrete cover in the constant moment zone, separated from the reinforcing bars like the beams that failed by interfacial shear failure of concrete. These two observations suggest that the inter-laminar shear failure in the CFRP sheet occurred just before the interfacial shear of concrete was reached.

Figure 45 shows that the load-deflection curve of Beam No. 11 is close to being bilinear while that of Beam No. 7 is curvilinear. This is because Beam No. 11 was pre-loaded and pre-cracked beyond yielding, prior to application of the CFRP sheet. Note that after inter-laminar shear failure, Beam No. 11 achieved the same loading capacity as the control beam, that is until the beam failed by compression failure of concrete in the top flange.

From these test results, it can be concluded that pre-loading and pre-cracking beyond reinforcement yielding have no serious influence on strengthening effect. Therefore, the CFRP glued-on sheet strengthening technique can be applied for flexural strengthening even to severely damaged beams.

3.7 Residual Strength of Beam after Failure

After failing by interfacial shear failure of concrete, and in order to check the residual strength, Beam No. 13 was unloaded and reloaded without any repair until the beam failed by compression failure of concrete. As shown in Figure 46, Beam No. 13 was severely damaged by delamination failure. The concrete cover in the constant moment zone was completely separated, and the two reinforcing bars in the lower layer were exposed to air. The bars had already yielded at time of delamination failure.

Figure 47 shows that Beam No. 13 attained the same ultimate load as the control beam even after severe damage by delamination. This fact is due to the two reinforcing bars in the lower layer which resisted the applied load because they had good bond in the shear span, even though they had lost bond in the constant moment zone. This result can be used as to provide a minimum safety level for strengthened beams, after failure of their CFRP sheet or plate.

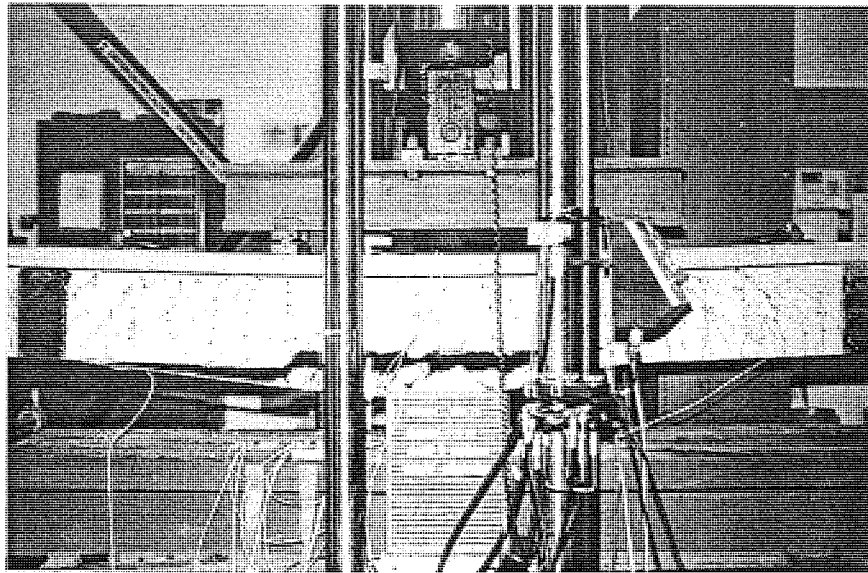


Figure 46 Condition of Beam No. 13 failed by delamination before re-testing.

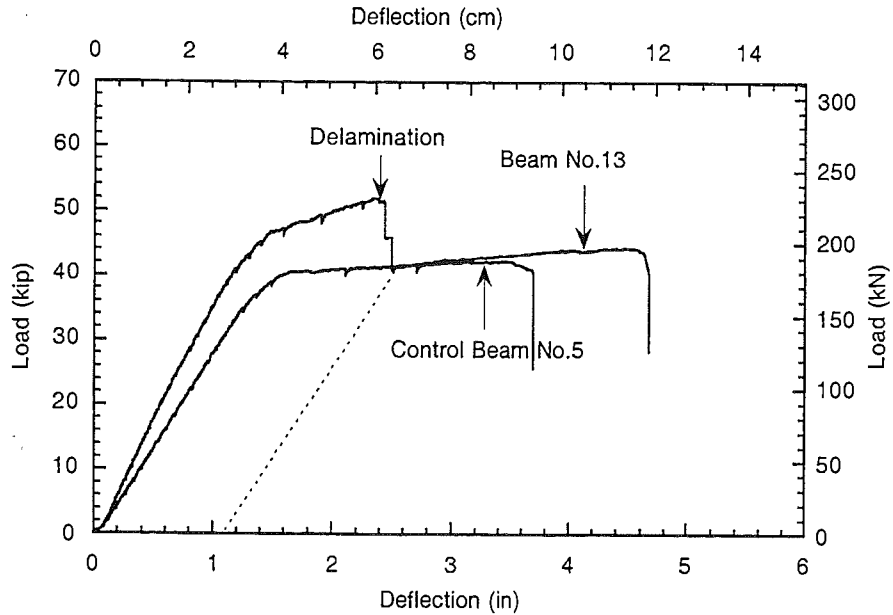


Figure 47 Load-deflection curves of Beam No. 13.

4. CONCLUSIONS

This investigation dealt with the flexural behavior of reinforced concrete beams strengthened using glued-on carbon fiber reinforced plastic (CFRP) sheets or plates. Based on the observation and analysis of the experimental test results the following conclusions can be drawn.

- 1) The strengthening technique using externally bonded CFRP sheets or plates can significantly improve the ultimate loading capacity of reinforced concrete beams; however, their ultimate deflection is reduced. On the other hand, the strengthened beams had, after failure or delamination of the CFRP sheets, a minimum loading capacity and ductility which were almost same as those of the control beam.
- 2) Strengthening with CFRP sheets can inhibit the growth of large cracks by helping distribute a large number of smaller cracks; it also protect the steel reinforcement from further corrosion.

- 3) In general, normally strengthened beams fail by interfacial shear failure (delamination) within the concrete, instead of by tensile failure of the CFRP sheet or plate.
- 4) In normally strengthened beams, the increment in ultimate load obtained by strengthening was almost proportional to the strengthening level or number of CFRP sheets. However, this direct relationship should be further confirmed experimentally in beams with higher strengthening levels and higher reinforcement ratios.
- 5) For a given reinforcement ratio, the ultimate load capacity increases with the strengthening level, or the number of CFRP sheets. However, the steel reinforcement ratio of the reinforced concrete beam to be strengthened, does not seem to have a significant effect on the increment of load at ultimate achieved by strengthening. This implies that the lower the reinforcement ratio, the higher the strengthening effect in terms of percent increase in ultimate load capacity.
- 6) The ultimate deflection of strengthened beams decreased in comparison to the control beam as the strengthening level increased, thus leading to a lower ductility. This is one of the disadvantages of beams strengthened using CFRP sheets. However, the strengthened beams had, after failure or delamination of the CFRP sheets, a minimum loading capacity and ductility which were almost same as those of the control beam.
- 7) Beams using the strengthening system with CFRP plate (Sika system) showed the same load versus deflection response as beams using the strengthening system with CFRP sheet (Tonen system), even though the tensile modulus of the CFRP plate was two thirds that of the CFRP sheet. In this investigation where non-trained students were involved, it was found that the system using CFRP plate is easier and more convenient for flexural strengthening than that using the CFRP sheet.
- 8) The strengthened beam with a smaller concrete cover had slightly higher ultimate load and considerably larger ultimate deflection than the control beam with normal concrete cover.

- 9) The beam strengthened after having a repaired concrete cover failed by gradual interlaminar debonding at the interface between existing concrete and repair mortar; it led to a ductile behavior, but did not achieve an adequate level of strengthening.
- 10) Using a U-shaped end anchorage of the CFRP sheet did not help attain higher ultimate loads or deflections, in comparison to having no anchorage. However, extending the sheet up to the supports led to slightly higher ultimate load and deflection. Therefore, the extended end anchorage system is recommended because it is easier to apply.
- 11) Preparing the concrete surface by grinding prior to the application of CFRP sheets was not more effective than simply vacuum cleaning and wiping the surface. However this conclusion should be further confirmed in real beams with deteriorated concrete surfaces.
- 12) Pre-loading and pre-cracking a beam beyond reinforcement yielding had no serious influence on the strengthening effect. Therefore, the CFRP glued-on strengthening technique can be applied even to severely damaged beams.
- 13) The beam that failed by CFRP sheet delamination and was damaged due to severe concrete cover spalling had, upon reloading, the same ultimate load and deflection as the control beam, even though the damage was severe. This fact can insure some minimum safety level for beams strengthened using CFRP sheets, should failure by delamination or tension of the sheet occur.
- 14) Based on the limited number of tests carried out, it seems that the contribution of the shear resistance of concrete to the strength of the interface linearly increases with the strengthening level. For this conclusion, the interface shear stress of concrete was calculated based on the assumption of equal shear stress along the shear span.

5. REFERENCES WITH SOURCE CLASSIFICATION (BENDING)

SOA - State of the Art Reports & Review Documents

- SOA-1. "State-of-the-art Report on Fiber Reinforced Plastic (FRP) Reinforcement for Concrete Structures". ACI Committee 440, 1996.
- SOA-2. "US Research Projects", International Research on Advanced Composites for construction (IRACC-96), Bologna, June 9-11, 1996.

FTS - Tonen Corp., H.S. Kliger & Associates. Structural Preservation Systems

- FTS-1. Kobayashi A., Endoh M., Kuroda H., Kliger H., "Use of Carbon Fiber Tow Sheet Reinforcement for Improved Bridge Capacity Ratings in Japan", 40th International SAMPE Symposium and Exhibition, Anaheim CA, May 8-11, 1995.
- FTS-2. Kobayashi A., Ohori N., Kuroda H., "Repair and Reinforcement of Concrete Structure With Carbon Fiber Tow Sheet", International Symposium on Non-metallic (FRP) Reinforcements for Concrete Structures, FRPCS-2, 23-25 August 1995, Ghent, Belgium.
- FTS-5. Yoshizawa H., Myojo T., Okoshi M., Mizukoshi M., Kliger H.S., "Effect Of Sheet Bonding Condition On Concrete Members Having Externally Bonded Carbon Fiber Sheet", Materials for the New Millennium. Proceedings of the Fourth Materials Engineering Conference. Washington D.C. Nov. 10-14, 1996, pp.1608-1616.

MRK - Mitsubishi (Replark). Craig Ballinger & Associates

- MRK-1. Nakamura M., Sakai H., Yagi K., Tanaka T., "Experimental Studies On The Flexural Reinforcing Effect Of Carbon Fiber Sheet Bonded To Reinforced Concrete Beam", pp760-773.

EMPA - Swiss Federal Laboratories for Materials Testing and Research

- EMPA-1. Meier U., "Strengthening of Structures Using Carbon Fiber/Epoxy Composites", Construction and Building materials, Vol.9, No.6, pp.341-351, 1995.

AZ -University of Arizona

- AZ-1. Saadatmanesh H., "Fiber Composites for New and Existing Structures", ACI Structural Journal, Vol.91, No.3, May-June 1994.
- AZ-2. Char M.S., Saadatmanesh H., Ehsani M.R., "Concrete Girders Externally Prestressed With Composite Plates", PCI Journal, May-June 1994, pp.40-51.
- AZ-3. Saadatmanesh H., Ehsani M.R., "RC Beams Strengthened with GFRP Plates. I: Experimental Study", Journal of Structural Engineering, Vol.117, No.11, Nov, 1991, pp.3417-3433.

DE - University of Delaware. Delaware Department of Transportation

- DE-1. Chajes M.J., Thomson T.A., Januszka T.F., Finch W.W., "Flexural Strengthening Of Concrete Beams Using Externally Bonded Composite Materials". 1994.

OH - Ohio Department of Transportation. Wright Patterson Air Force Base.
University of Dayton Research Institute. Ohio State University

- OH-1. Morton S.E., Schaefer K.R., Mistretta J., "Research On Externally Applied Fiber Reinforced Plastics For Rehabilitation Of Concrete And Steel Bridges", Ohio Department of Transportation, Bureau of Bridges, 5-24-95, pp.2+12.
OH-2. Crasto A.S., Kim R.Y., Fowler C., Mistretta J., "Rehabilitation of Concrete Bridge Beams with Externally-Bonded Composite Plates. Part I", pp.857-869.

WVU - West Virginia University, Constructed Facilities Center

- WVU-1. Faza S.S., GangaRao H.V.S., Barbero E.J., "Fiber Composite Wrap for Rehabilitation of Concrete Structures", Conf. On The Repair and Rehabilitation of the Infrastructure of the Americas, University of Puerto Rico, Mayaguez, August 1994, pp.181-192.

RNJ - RUTGERS The State Univ. of New Jersey. GEOPOLYMERE

- RNJ-1. Balaguru P., Kurtz S., Rudolph J., "Geopolymer For Repair And Rehabilitation Of Reinforced Concrete Beams", Internet,
http://www.insset.u-picardie.fr/geopolymer/fichiers_pdf/REINFORC.pdf.

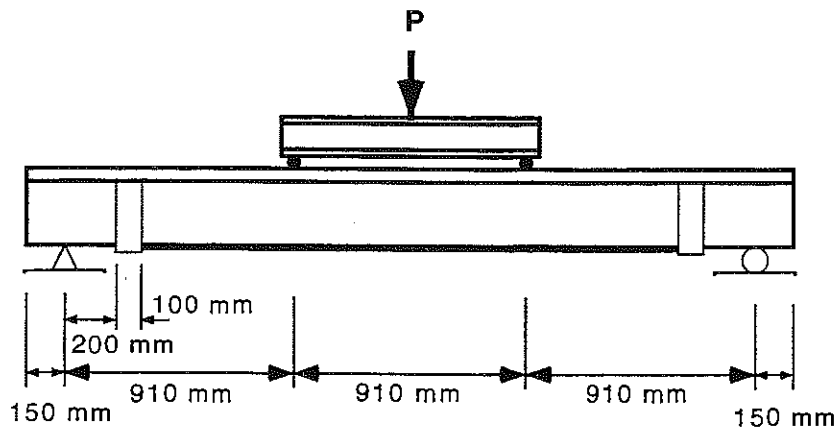
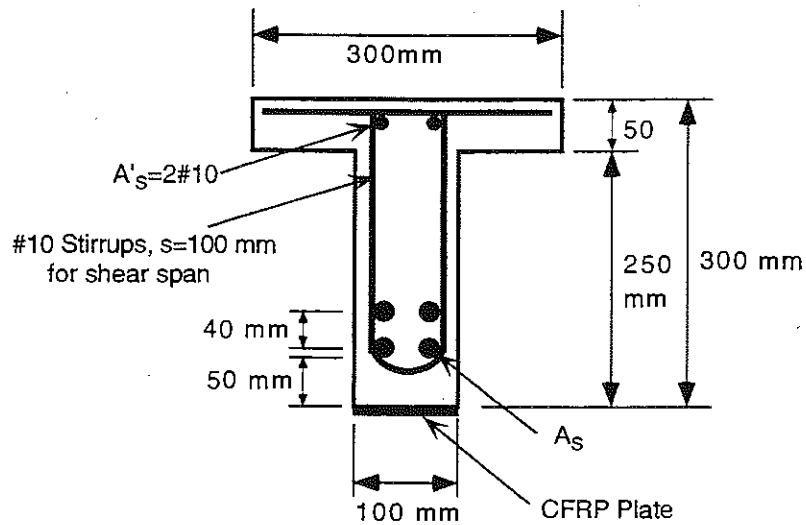
XX - Other Research Institutions

- XX-1. M'Bazaa I., Missihoun M., Labossiere P., "Strengthening of Reinforced Beams with CFRP Sheets", 1st International Conference Composites in Infrastructure, ICCI, Tucson, Arizona, January 1996, pp.746-759.
XX-2. Malvar L.J., Warren G.E., Inaba C., "Rehabilitation of Navy Pier Beams with Composite Sheets", International Symposium on Non-metallic (FRP) Reinforcements for Concrete Structures, FRPCS-2, 23-25 August 1995, Ghent, Belgium.
XX-3. Inaba C.M., Warren G.E., Malvar L.J., "Rehabilitation of Navy Pier Decks with Composite Sheets", 1st International Conference Composites in Infrastructure, ICCI, Tucson, Arizona, January 1996, pp.1193-1201.
XX-4. Malvar L.J., Warren G.E., Inaba C., "Composite Applications In The NAVY Waterfront Infrastructure", Materials for the New Millennium. Proceedings of the Fourth Materials Engineering Conference. Washington D.C. Nov. 10-14, 1996. Pp.1179-1188.
XX-5. Sharif A., Al-Sulaimani G.J., Basunbul I.A., Baluch M.H., Ghaleb B.N., "Strengthening of Initially Loaded Reinforced Concrete Beams Using FRP Plates", ACI Structural Journal, Vol.91, No.2, March-April 1994, pp.160-168.

- XX-6. Sharif A., Baluch M.H., "External FRP Plates to Strengthen Reinforced Concrete Beams", 1st International Conference Composites in Infrastructure, ICCI, Tucson, Arizona, January 1996, pp.814-828.
- XX-37. Ritchie Philip A., Thomas David A., Lu Le-Wu, and Connelly Guy M., "External Reinforcement of concrete Beams using Fiber Reinforced Plastics," ACI Structural journal, vol. 88, July-August 1991, pp. 490-500.

6. APPENDIX A

Moment Capacity Calculations



- Distance from centroid of steel to top layer of concrete

For beam No.1-4:

$$d_1 = (12 - 2 \cdot 4/8 \cdot 1/2) \cdot 25.4 = 248 \text{ mm}, \quad d_2 = (12 - 2 \cdot 4/8 \cdot 1/2 - 1.5) \cdot 25.4 = 210 \text{ mm}$$

$$d_e = (9.75 \cdot 0.2^2 + 8.25 \cdot 0.11^2) / 0.62 \cdot 25.4 = 235 \text{ mm}$$

For beam No. 5-14:

$$d_1 = (12 - 2 \cdot 5/8 \cdot 1/2) \cdot 25.4 = 246 \text{ mm}, \quad d_2 = (12 - 2 \cdot 5/8 \cdot 1/2 - 1.5) \cdot 25.4 = 208 \text{ mm}$$

$$d_e = (d_1 + d_2) / 2 = 227 \text{ mm}$$

- Concrete compressive strength = 55.2 MPa , $\beta_1 = 0.65$

- Steel yield strength:

For bars #10 & #13, $f_y = (73 \cdot 0.11 + 62 \cdot 0.2) / 0.31 \cdot 6.895 = 455 \text{ MPa}$

For #16 bar, $f_y = 455 \text{ MPa}$

- As balance

T-section behavior: As balance = Concrete force due to equilibrium (C_c) / f_y

For $d_e = 227 \text{ mm}$, c_d (neutral axis) for balance condition = $134 \text{ mm} >$ flange height ($h_f = 51 \text{ mm}$). Find C_c for T-section:

$$C_c = (b - b_w) \cdot h_f \cdot 0.85 \cdot f_c + 0.85 \cdot f_c \cdot b_w \cdot \beta_1 \cdot C_d$$

$$C_c = 900 \text{ kN}$$

$$\text{As balance} = 900,000 / 455 = 1977 \text{ mm}^2, \text{As}_{\max} = 0.75 \text{ As balance} = 1483 \text{ mm}^2$$

For $d_e = 235 \text{ mm}$, c_d (neutral axis) for balance condition = $139 \text{ mm} >$ flange height (51 mm). Find C_c for T-section:

$$C_c = (b - b_w) \cdot h_f \cdot 0.85 \cdot f_c + 0.85 \cdot f_c \cdot b_w \cdot \beta_1 \cdot C_d$$

$$C_c = 914 \text{ kN}$$

$$\text{As balance} = 914,000 / 455 = 2000 \text{ mm}^2, \text{As}_{\max} = 0.75 \text{ As balance} = 1506 \text{ mm}^2$$

Take $\text{As}_{\max} = 1490 \text{ mm}^2$

- M_{\max}

$M_{\max} = \text{As}_{\max} \cdot f_y \cdot (d_e - a/2)$, where $a = \text{As}_{\max} \cdot f_y / (0.85 \cdot f_c \cdot b_f)$ if $a > h_f$ T-section behavior. This equation can not be applied.

For $d_e = 227 \text{ mm}$, $a = 47 \text{ mm} < 51 \text{ mm}$, Rectangular (R) beam behavior,

$$M_{\max} = 138 \text{ kN-m}$$

For $d_e = 235 \text{ mm}$, $a = 47 \text{ mm} < 51 \text{ mm}$, R-behavior, $M_{\max} = 143 \text{ kN-m}$

- M_n

$M_n = \text{As} \cdot f_y \cdot (d_e - a/2)$, where $a = \text{As} \cdot f_y / (0.85 \cdot f_c \cdot b_f)$ if $a > h_f$ T-section behavior. This equation can not be applied.

For $\text{As} = 400 \text{ mm}^2$, $d_e = 235 \text{ mm}$, $a = 13 \text{ mm} < 51 \text{ mm}$, R-behavior! $M_n = 42 \text{ kN-m}$

For $\text{As} = 800 \text{ mm}^2$, $d_e = 227 \text{ mm}$, $a = 25 \text{ mm} < 51 \text{ mm}$, R-behavior! $M_n = 78 \text{ kN-m}$

- M_{As} , M_{FRP}

For beam No. 1-4:

1 layer CFRP

$$T_{As} = 0.62 \cdot 66 \cdot 4.448 = 182 \text{ kN}$$

$$T_{FRP} = 3.28 \cdot 4 \cdot 4.448 = 58.36 \text{ kN}$$

$$T_{total} = 240.55 \text{ kN}$$

$$a = T_{total} / (0.85 \cdot f_c \cdot b \cdot f) = 16.8 \text{ mm}$$

$$M_{As} = T_{As} \cdot (d_e - a/2) = 41.09 \text{ kN-m}$$

$$M_{FRP} = T_{FRP} \cdot (h - a/2) = 17.30 \text{ kN-m}$$

$$M_{(As + FRP)} = M_{As} + M_{FRP} = 58.39 \text{ kN-m}$$

2 layers CFRP

$$T_{As} = 0.62 \cdot 66 \cdot 4.448 = 182 \text{ kN}$$

$$T_{FRP} = 3.28 \cdot 8 \cdot 4.448 = 116.7 \text{ kN}$$

$$T_{total} = 298.73 \text{ kN}$$

$$a = T_{total} / (0.85 \cdot f_c \cdot b \cdot f) = 20.8 \text{ mm}$$

$$M_{As} = T_{As} \cdot (d_e - a/2) = 40.73 \text{ kN-m}$$

$$M_{FRP} = T_{FRP} \cdot (h - a/2) = 34.35 \text{ kN-m}$$

$$M_{(As + FRP)} = M_{As} + M_{FRP} = 75.08 \text{ kN-m}$$

4 layers CFRP

$$T_{As} = 0.62 \cdot 66 \cdot 4.448 = 182 \text{ kN}$$

$$T_{FRP} = 3.28 \cdot 16 \cdot 4.448 = 233.43 \text{ kN}$$

$$T_{total} = 415.44 \text{ kN}$$

$$a = T_{total} / (0.85 \cdot f_c \cdot b \cdot f) = 29 \text{ mm}$$

$$M_{As} = T_{As} \cdot (d_e - a/2) = 40 \text{ kN-m}$$

$$M_{FRP} = T_{FRP} \cdot (h - a/2) = 67.77 \text{ kN-m}$$

$$M_{(As + FRP)} = M_{As} + M_{FRP} = 107.77 \text{ kN-m}$$

For beam No. 5-14:

1 layer CFRP

$$T_{As} = 1.24 \cdot 66 \cdot 4.448 = 364 \text{ kN}$$

$$T_{FRP} = 3.28 \cdot 4 \cdot 4.448 = 58.36 \text{ kN}$$

$$T_{total} = 128.74 \text{ kN}$$

$$a = T_{\text{total}} / (0.85 \cdot f_c \cdot b \cdot f) = 29.5 \text{ mm}$$

$$M_{\text{As}} = T_{\text{As}} \cdot (d_e - a/2) = 77.30 \text{ kN-m}$$

$$M_{\text{FRP}} = T_{\text{FRP}} \cdot (h - a/2) = 16.93 \text{ kN-m}$$

$$M_{(\text{As} + \text{FRP})} = M_{\text{As}} + M_{\text{FRP}} = 94.24 \text{ kN-m}$$

2 layers CFRP

$$T_{\text{As}} = 1.24 \cdot 66 \cdot 4.448 = 364 \text{ kN}$$

$$T_{\text{FRP}} = 3.28 \cdot 4 \cdot 4.448 = 116.7 \text{ kN}$$

$$T_{\text{total}} = 480.74 \text{ kN}$$

$$a = T_{\text{total}} / (0.85 \cdot f_c \cdot b \cdot f) = 33.5 \text{ mm}$$

$$M_{\text{As}} = T_{\text{As}} \cdot (d_e - a/2) = 76.59 \text{ kN-m}$$

$$M_{\text{FRP}} = T_{\text{FRP}} \cdot (h - a/2) = 33.62 \text{ kN-m}$$

$$M_{(\text{As} + \text{FRP})} = M_{\text{As}} + M_{\text{FRP}} = 110.18 \text{ kN-m}$$

25 mm cover & 2 CFRP layers

$$M_{\text{As}} = T_{\text{As}} \cdot (d_e - a/2) = 76.59 \text{ kN-m}$$

$$M_{\text{FRP}} = T_{\text{FRP}} \cdot (h - 25 - a/2) = 30.65 \text{ kN-m}$$

$$M_{(\text{As} + \text{FRP})} = M_{\text{As}} + M_{\text{FRP}} = 107.21 \text{ kN-m}$$

Sika. b=38 mm

$$T_{\text{As}} = 364 \text{ kN}$$

$$T_{\text{FRP}} = 109.15 \text{ kN}$$

$$T_{\text{total}} = 473.18 \text{ kN}$$

$$a = T_{\text{total}} / (0.85 \cdot f_c \cdot b \cdot f) = 33 \text{ mm}$$

$$M_{\text{As}} = T_{\text{As}} \cdot (d_e - a/2) = 76.65 \text{ kN-m}$$

$$M_{\text{FRP}} = T_{\text{FRP}} \cdot (h - a/2) = 31.47 \text{ kN-m}$$

$$M_{(\text{As} + \text{FRP})} = M_{\text{As}} + M_{\text{FRP}} = 108.12 \text{ kN-m}$$

Sika. b=102 mm

$$T_{\text{As}} = 364 \text{ kN}$$

$$T_{\text{FRP}} = 291.08 \text{ kN}$$

$$T_{\text{total}} = 655.10 \text{ kN}$$

$$a = T_{\text{total}} / (0.85 \cdot f_c \cdot b \cdot f) = 45.7 \text{ mm}$$

$$M_{\text{As}} = T_{\text{As}} \cdot (d_e - a/2) = 74.06 \text{ kN-m}$$

$$M_{\text{FRP}} = T_{\text{FRP}} \cdot (h - a/2) = 82.06 \text{ kN-m}$$

$$M_{(\text{As} + \text{FRP})} = M_{\text{As}} + M_{\text{FRP}} = 156.13 \text{ kN-m}$$